NATIONAL ADVISORY COMMITTEE FOR AERONAUTICS

TECHNICAL NOTE

No. 1785

FRICTION COEFFICIENTS IN THE INLET LENGTH OF SMOOTH ROUND TUBES

By Ascher H. Shapiro and R. Douglas Smith

Massachusetts Institute of Technology

Washington
November 1948

NATIONAL ADVISORY COMMITTEE FOR AERONAUTICS

TECHNICAL NOTE NO. 1785

FRICTION COEFFICIENTS IN THE INLET LENGTH OF SMOOTH, ROUND TUBES

By Ascher H. Shapiro and R. Douglas Smith

SUMMARY

An experimental study was made of friction coefficients near the inlet of smooth, round tubes with bellmouth entrances. The range of Reynolds number (based on tube diameter) was from 39,000 to 590,000; these values corresponded to turbulent flow in the region of a fully developed velocity profile. The tube size ranged from 3/8 inch to 4 inches. Four different combinations of approach section and bellmouth entry were used. Tests were made both with water and with air at low Mach numbers.

The results are reported in terms of the apparent friction coefficient, which is directly a measure of the pressure drop and which includes the effects of both friction and of changes in momentum flux associated with changes in velocity profile.

Near the inlet the tests indicated a zone in which the developing boundary layer is laminar, followed by a zone in which the boundary layer is turbulent. Transition from a laminar to turbulent boundary layer was found to occur at a Reynolds number (based on distance from the tube inlet) of about 5×10^5, which compares well with the corresponding value for a flat plate.

In the inlet region the friction coefficient was found to vary widely from the Kármán-Nikuradse coefficient for fully developed turbulent flow and was sometimes greater and sometimes less than the Kármán-Nikuradse value, depending on the value of the Reynolds number. About 50 tube diameters were required for the local friction coefficient to come within 5 percent of the Kármán-Nikuradse value and about 80 diameters for the integrated friction coefficient to come within 5 percent of the Kármán-Nikuradse value.

The effects of inducing turbulence artifically by wire screens and by an obstruction on the tube wall were studied.

In the laminar inlet zone the results were found to be in accord with the theory of Langhaar.

Values of the friction coefficient measured at large distances from the tube inlet were found to be systematically about 1.3 percent higher than the values given by the Kármán-Nikuradse formula.

An approximate method for predicting the discharge coefficient of rounded-entrance flow nozzles, based on the reported results, is presented and is shown to compare well with published data on flow nozzles.

INTRODUCTION

General

When a fluid flows steadily through a tube, the flow pattern in the region immediately downstream of the entrance to the tube depends in great degree on the distance from the tube entrance. After this distance has become sufficiently great, that is, of the order of 50 tube diameters in length, the variations in flow pattern vanish, the velocity profile remains unaltered, and the friction coefficient is independent of the distance from tube inlet.

The changes in velocity profile which occur in the inlet region immediately downstream of the tube entrance have an important effect on the friction coefficient in this region. Through the combined efforts of many investigators the values of the friction coefficient in the permanent zone downstream of the inlet region have been established with good accuracy. For the inlet zone, on the other hand, only scant and inconclusive data are available.

There are many instances in the design of engineering equipment, particularly aircraft equipment, where the length-diameter ratios of ducts and of tubes are not large compared with the length-diameter ratio in which inlet effects are strong. As instances may be cited the following cases:

(a) The tubes of radiators, intercoolers, and oil coolers

(b) The ducts connecting air scoops in aircraft with cooling equipment or propulsion devices

(c) The passageways in ram-jet and gas-turbine power plants

(d) The connecting and return ducts for wind tunnels.

Object

The object of this investigation was to determine experimentally the values of the friction coefficient in the inlet length of round, straight, smooth tubes and to find the effects on the friction coefficient of Reynolds number, distance from the entrance, and initial turbulence. The range of Reynolds number was to correspond to turbulent flow in the fully developed region, and compressibility effects were to be eliminated as a complicating factor by making tests with water and with air at very low Mach numbers.

Historical Background

Analytical.- Boussinesq (reference 1), in 1890, employed an approximate form of the Navier-Stokes equation to obtain a solution for the development of the velocity profile for laminar flow in round tubes. His results led to a predicted length-diameter ratio for a purely laminar inlet zone of

$$(x/D)_{inlet} = 0.065R_D$$

Schiller (reference 2) investigated the laminar inlet zone with the aid of Kármán's momentum theory for the boundary layer. After assuming that the typical velocity profile near the inlet was composed of a straight-line segment terminated by parabolic arcs, he applied the momentum equation to the entire cross section and the Bernoulli equation to the central, frictionless core of fluid. The rate of development of the velocity profile was computed, in addition to which the pressure drop from the entrance was predicted. For the length of a purely laminar inlet zone he obtained

$$(x/D)_{inlet} = 0.029R_D$$

Atkinson and Goldstein (reference 3), also using an approximate form of the Navier-Stokes equation, improved upon the results of Boussinesq by employing near the entry a series solution based in part on a generalization of the Blasius boundary-layer equation.

Langhaar (reference 4) presented the most complete analysis for laminar flow. He retained more terms of the Navier-Stokes equation than had been retained by other investigators and obtained a solution by a linearizing procedure which can be partially justified on theoretical grounds. His results are in the form of tables from which velocity profiles

and pressure drops may be computed. Unlike the previous work in this field, no definite inlet length was found, but instead the velocity profile was found to approach the parabolic form of Poiseuille in asymptotic fashion. The length in which the center-line velocity reaches 99 percent of its asymptotic value was predicted to be

$$(x/D)_{99 \text{ percent inlet}} = 0.115R_D$$

Latzko (reference 5) analyzed the development of a turbulent velocity profile in a tube by a method analogous to that of Schiller (reference 2). The basic assumption of Latzko's analysis was that a typical velocity profile in the inlet length is composed of a straight-line segment terminated by arcs, the velocity distribution of which follows the one-seventh-power law. For the total inlet length of a purely turbulent flow he obtained

$$(x/D)_{inlet} = 0.693R_D^{0.25}$$

Experimental.- Kirsten (reference 6) measured velocity profiles at various distances from bellmouth and sharp-edged entrances for the flow of air through smooth tubes at very low Mach numbers and over a range of Reynolds number (based on tube diameter) from 20,000 to 80,000. In the case of flow with a well-rounded entrance, the nature of the velocity profiles seemed to indicate that the boundary layer near the entrance is at first laminar and that at some distance from the inlet a transition occurs to the type of combined laminar and turbulent layer customarily associated with flow over a flat plate and with fully developed turbulent flow in a pipe. Kirsten also made a few static-pressure measurements at the tube wall and was able to compute friction coefficients for two Reynolds numbers.

Nikuradse (see reference 7, p. 27) reported velocity profiles for a purely laminar inlet region. (Reference 7 gives only a set of curves attributed to Nikuradse; a detailed account appears not to have been published.) A comparison of these measurements with the theories of Boussinesq (reference 1), Schiller (reference 2), Atkinson and Goldstein (reference 3), and Langhaar (reference 4) indicates, at least on the basis of center-line velocities, that Langhaar's treatment is most correct physically over the entire inlet region. The method of Schiller predicts center-line velocities accurately at points close to the entry and poorly at points near the end of the inlet zone. The methods of Boussinesq and of Atkinson-Goldstein, on the other hand, compare well with Nikuradse's measurements near the end of the inlet region and compare poorly near the entry of the duct.

The experimental results for water flow reported herein for tube I were obtained by Brooks, Craft, and Montrello (reference 8).

The experimental results for air flow reported herein for tube IV were obtained by Smith (reference 9).

This present project was carried out in the Mechanical Engineering Department of the Massachusetts Institute of Technology under the sponsorship and with the financial assistance of the National Advisory Committee for Aeronautics. The work was carried on during 1943-44 and during 1946-47.

The help and encouragement of Professor J. H. Keenan, particularly in the early stages, are acknowledged with thanks.

Mr. William Vaismann gave valuable assistance in taking and reducing data.

SYMBOLS

A	cross-sectional area of tube, square feet
c_w	discharge coefficient for flow nozzle, defined by equation (11), dimensionless
D	diameter of tube, feet
f_{APP}	local apparent friction coefficient, defined by equation (4), dimensionless
f_{APP}	integrated apparent friction coefficient, defined by equations (5) and (6), dimensionless
f_{DEV}	friction coefficient in region of unchanging velocity profile, dimensionless
f_{K-N}	friction coefficient from Kármán-Nikuradse formula (equation 7) corresponding to value of R_D
p	static pressure, pounds per square foot
R_D	Reynolds number, dimensionless $(VD\rho/\mu)$
R_x	Reynolds number, dimensionless $(Vx\rho/\mu)$

V mean velocity, feet per second

w mass rate of flow, slugs per second

x distance from beginning of cylindrical part of tube, feet

μ viscosity, slugs per foot-second

ρ density, slugs per cubic foot

THEORETICAL CONSIDERATIONS

The usual procedure in calculating friction coefficients from pressure-drop data is to assume that the velocity is uniform over each cross section. Since this ignores the changes in momentum flux which accompany a change in velocity profile, it follows that such a friction factor does not represent the true drag coefficient, or, in other words, it is not equal to the ratio of the shearing stress at the wall to the velocity head of the stream. Friction coefficients calculated in this simple way are therefore called "apparent friction coefficient." In order to calculate the "true friction factor," that is, the ratio of the wall shearing stress to the velocity head, it is necessary to consider not only the pressure drops involved but also the changes in velocity profile. The true friction factor is identical with the apparent friction factor only when the velocity distribution is the same at all cross sections considered and when the flow is incompressible.

When the tube has a well-rounded entrance the formation of the boundary layer might reasonably be expected to be similar to the boundary-layer growth near the leading edge of the flat plate. For a short distance from the entrance the boundary layer would be laminar. Then, at some distance from the leading edge presumably dependent on the degree of initial turbulence, the outer portion of the boundary layer would become turbulent. The turbulent boundary layer would then spread until it reached the center of the tube, following which the velocity profile would asymptotically approach the shape corresponding to fully developed turbulent flow.

The nature of viscous (laminar) flow, the stability of laminar flow, and the mechanism of turbulence are all associated with the Reynolds number. Furthermore, the amount and structure of turbulence in the stream at the tube entrance doubtless have an influence on the location at which the transition to turbulence occurs and on the manner in which the turbulent velocity profile develops. Both Reynolds number and initial turbulence, therefore, might be expected to have an effect on the friction coefficient in the transition region.

It was early decided in this investigation to measure apparent friction coefficients rather than true friction coefficients. This decision was prompted first, by the fact that the designer is interested primarily in apparent friction coefficients, and second, by the manifold greater complexity of the apparatus required to measure true friction coefficients.

APPARATUS AND TEST PROCEDURE

On the basis of the considerations just outlined, the tests were carried out with water and with air at low Mach numbers. The principal data comprised measurements of flow rates, static pressures and pressure differences at the wall of the duct, and inlet temperatures.

Four different test ducts were used. Those used for the water tests are identified as tubes I, II, and III, and the single duct used for the air tests is tube IV. The principal dimensions, nature of entry section, and size and location of pressure taps for these tubes are shown in figure 1 and in table I.

Because of the emphasis on the region of changing velocity distribution, the pressure taps were most numerous and most closely spaced near the entrance of each tube.

Water Tests

Flow system.- Water was drawn from a large header supplied by a centrifugal pump at a pressure ranging from about 100 to 200 pounds per square inch gage, through a hand-controlled throttle valve, through the approach section to the test pipe, and, after passing through the test pipe, was discharged into an open weighing tank. The usual variations in flow rate during a test were of the order of 1 percent or less.

Design of tubes.- Tube I, which had an inside diameter of 0.373 inch, was attached by a reducing bushing to a straight run of 18 feet (85 diameters) of $2\frac{1}{2}$-inch, black iron pipe. The reducing bushing was machined on the inside to provide a smooth passage for the flow. Upstream of the 18-foot run was a 2-foot section of $2\frac{1}{2}$-inch pipe filled with straightening vanes. The entrance to the test duct proper was, in cross section, a circular arc with a radius approximately equal to the diameter of the test section, that is, 3/8 inch. Brass was used for the test duct and all attached fittings. Pressure taps were cleanly drilled through the tube wall, and great care was exercised to insure that the taps were square and without

burrs on the inside of the tube. Connections were made to the pressure taps by means of saddles soldered to the test pipe.

The test pipe with its attached bellmouth inlet used for tube II was the same one as that used for tube I. The sole difference between the tests with tube I and with tube II lay in the approach section used for the respective tests. For the tests with tube II, the 10-inch calming chamber shown in figure 1(a) was placed upstream of the test pipe, as shown in figure 1(c). The baffles, honeycomb, and screens in this stilling section, together with the area reduction of 700:1 between the stilling section and test duct, would, it was believed, reduce the initial turbulence in the test section to very small proportions.

Tube III, shown in figure 1(d), was of brass and of 0.735-inch internal diameter. Like tube II, it was attached to the stilling chamber of figure 1(a), the corresponding area reduction being 185:1. In construction it was similar to tube I, except that at each of the first four pressure stations there were four pressure taps connected by a piezometer ring. This arrangement tended to reduce errors near the entrance which might be caused by a slight imperfection in a single pressure tap.

All the test pipes used in the investigation were polished on the inside. The diameters were carefully measured at as many locations and as many orientations as convenient. The average diameters of tubes I, II, and III over their entire lengths were found by filling with water. Departures from roundness and from uniformity in diameter were within 0.001 inch. The bellmouth entry was in each case machined while attached to the tube proper, and the inlet curve was burnished so that there was no observable junction between the bellmouth and the tube.

For runs with induced turbulence with tubes II and III, brass screening (24-mesh, 30-gage) was placed near the exit of the calming chamber, flush with the flange just prior to the bellmouth entry to the test duct.

Measurements.- Each of the pressure taps was connected through tubing and shutoff valves to two manifolds. Each manifold was connected in turn to each leg of a mercury-water U-tube manometer and an air-water U-tube manometer. With this manifold arrangement, pressure differences could be measured between any pair of taps, and the pressure taps could be reversed relative to the manifolds and to the manometers so as to permit tests for leakage in all parts of the system. Because of the important effects that even the smallest amount of leakage might have had on the measurements, every set of readings was checked for leakage by reversal of the connections between the pressure taps and the manifolds. All connection lines were carefully purged of air and filled with water prior to each test.

Flow rates were measured by direct weighing in an open tank mounted on platform scales.

Auxiliary measurements included the temperature of the water leaving the apparatus, the pressure in the calming chamber, the pressure in the manifolds to permit corrections for the head of air in the air-water manometer, atmospheric temperature, and atmospheric pressure.

Air Tests

Flow system.- Air was drawn at atmospheric pressure from a large room into the test pipe through the bellmouth entry shown in figure 1(e). After leaving the test duct, the air passed through a sharp-edged orifice meter and was then discharged outside the building by a steam ejector.

During each run at a specified Reynolds number the flow rate was maintained nearly constant by manual control of a throttle valve downstream of the orifice meter.

Design of tube.- Tube IV was of copper with an internal diameter of 4 inches. The entry consisted of a spun-copper bellmouth attached to an annular disc of plywood 34 inches in diameter. The bellmouth was in cross section an ellipse having the dimensions shown in figure 1(e). Presumably the air drawn from a large quiet room into the test pipe through this bellmouth was very nearly free of measurable turbulence.

The precautions followed for tubes I, II, and III in obtaining clean and square pressure taps, a smooth finish on the inside of the pipe, and a smooth, continuous juncture between pipe and bellmouth, were followed also in the case of tube IV.

For runs with induced turbulence, two different methods of creating turbulence were employed: (a) A piece of brass screening 4 inches in diameter (24-mesh, 30-gage) was placed in the test duct at the end of the bellmouth entry where the latter joined onto the cylindrical test pipe and (b) a piece of scotch tape 1/4 inch wide and 0.0033 inch thick was placed around the inside periphery of the duct at the same location as the aforementioned screening.

Measurements.- The first pressure tap was connected to a water-micromanometer. Each of the other pressure taps was connected through a length of tubing and a valve to a manifold, and the latter was connected to a second micromanometer. Both micromanometers had one leg open to the atmosphere. Pressure differences were in each case measured between the first tap and the atmosphere and between each of the succeeding taps and

the atmosphere, so that the pressure drop between any pair of taps could be found by subtraction. All joints and connections were covered with glyptol so as to avoid leakage insofar as possible.

The flow rate was calculated from the pressure and temperature upstream of the sharp-edged orifice, the pressure drop across the orifice as measured with a U-tube manometer, and standard A.G.A.-A.S.M.E. discharge coefficients (reference 10).

Measurements of the pressure and temperature of the air in the room which supplied air to the test duct were made throughout each run.

METHODS OF COMPUTATION

Definitions

Reynolds numbers.- The Reynolds number based on pipe diameter R_D is defined by

$$R_D = \frac{VD\rho}{\mu} \tag{1}$$

where V is the mean velocity with respect to mass rate of flow and the density ρ and viscosity μ are evaluated at the mean pressure and temperature of the stream.

The Reynolds number based on distance from the inlet R_x is defined by

$$R_x = \frac{Vx\rho}{\mu} \tag{2}$$

where x is the axial distance from the point where the cylindrical portion of the pipe begins (see fig. 1(c)).

From equations (1) and (2) it is evident that

$$R_x = R_D\,(x/D) \tag{3}$$

Friction coefficients.- The local apparent friction coefficient f_{APP} is defined by

$$p_2 - p_1 = 4f_{APP} \frac{x_2 - x_1}{D} \frac{\rho}{2} V^2 \tag{4}$$

where p_2 and p_1 are the static pressures (measured at the wall of the duct) at the axial locations x_2 and x_1, respectively. The value of f_{APP} calculated from equation (4) was taken to be the local value midway between stations 1 and 2, or, in other words, at the axial location $(x_1 + x_2)/2$. This type of friction coefficient includes the effects both of shearing stress at the wall and of changes in momentum flux associated with changes in velocity profile. When the velocity profile is the same at x_2 and x_1, the local apparent friction coefficient is identical with the true drag coefficient; it is then equal to $2\tau_w/\rho V^2$, where τ_w denotes the shearing stress at the wall. When the velocity profile is developing, it may be shown that the local apparent friction coefficient is always greater than the true drag coefficient.

The integrated apparent friction coefficient $\bar{f}_{APP}$ is similar to the local value f_{APP} but provides a measure of the total pressure drop from a fixed point near the beginning of the duct to any other point downstream. It is defined by

$$p - p^* = 4\bar{f}_{APP} \frac{x - x^*}{D} \frac{\rho}{2} V^2 \tag{5}$$

where the asterisk refers to the fixed point near the entrance of the duct. For design purposes it would be preferable to have x^* equal to zero. It was not possible to do this for the experimental tests because of the difficulty of obtaining a meaningful pressure measurement at the point where the bellmouth entry joins the cylindrical tube. In the tests with tube II, for which values of $\bar{f}_{APP}$ are reported, x^*/D was equal to unity. The theoretical results for laminar flow of Langhaar, Schiller, and Atkinson and Goldstein are based on x^*/D equal to zero.

By comparing equations (4) and (5), the following relation between the local and integrated apparent friction coefficients is obtained:

$$\bar{f}_{APP} = \frac{\int_{(x/D)^*}^{(x/D)} f_{APP}\, d(x/D)}{(x/D) - (x/D)^*} \tag{6}$$

The developed friction coefficient f_{DEV} is the value of the local friction coefficient at axial distances so great from the inlet that the effects of changing velocity profile are no longer observable. It is computed from equation (4). The value of f_{DEV} was assumed to be the same as f_{APP} when the variations with x/D of the latter were within the experimental accuracy.

The Kármán-Nikuradse friction coefficient f_{K-N} is based on the experimental research of Nikuradse (reference 11) and the analytical formulation of Von Kármán (reference 12). It is given by

$$\frac{1}{\sqrt{4f_{K-N}}} = -0.8 + 2 \log R_D \sqrt{4f_{K-N}} \qquad (7)$$

Precision

During each run at a specified Reynolds number, there were slight variations in flow rate. In order to eliminate the effects of these variations, all results were reduced to standard conditions for each run in terms of an average value of the measured pressure drop from the calming chamber to the first pressure tap. In making corrections it was assumed that the flow rate was proportional to the square root of the reference pressure drop and that pressure differences were directly proportional to the reference pressure drop. In no case did these corrections exceed 1 percent.

The average flow rates were, in the case of the water tests, accurate to about 0.2 percent and, for the air tests, to about 1 percent.

The reported friction coefficients for the water tests were, as regards precision of measurement, accurate to about 0.5 percent, except for two runs at low values of R_D, where the accuracy was about 1 percent. In the air tests, because of the small pressure drop between taps, the friction coefficients were accurate only to about 5 percent.

It is important to note, however, that the reported friction coefficients near the inlet are subject to a source of error entirely independent of the instrumentation, namely, the effects of nonuniformity in the different pressure taps. For example, the pressure drop between two taps 1 tube diameter apart is of the order of 2 percent of the velocity head; in that case a defect in one of the taps which produced an error in the measured pressure of only 0.1 percent of the velocity head would cause an error in the friction coefficient of 5 percent. The error is correspondingly larger for smaller tap spacings or for greater defects in the

pressure taps. Therefore, although the tubes were carefully polished with fine emery cloth on the inside so as to obtain clean pressure taps, appreciable errors due to imperfections in the taps are doubtless present near the inlets to the tubes. This is particularly true for tube IV, where the tap spacing was as small as $\frac{1}{2}$ tube diameter.

RESULTS AND DISCUSSION

Apparent Local Friction Coefficient

The results of the tests are given in figures 2 to 5 in the form of curves in which the ratio of the local apparent friction coefficient to the Kármán-Nikuradse coefficient is plotted against the ratio of the distance from the inlet to the tube diameter. Each curve is for a fixed value of R_D. Straight lines were used for joining the points because of the difficulty of fairing in smooth curves.

At first sight these charts seem to have no regularity whatsoever. Closer examination discloses, however, that at very low Reynolds numbers the friction-coefficient ratio at first decreases with distance from the inlet, then increases rather sharply, and, after a sharp drop followed sometimes by a slight rise, finally decreases relatively slowly until it approaches an asymptote of about unity. At intermediate Reynolds numbers the pattern is similar, except that over the experimental range of x/D values the initial decrease in the friction-coefficient ratio is absent. At the highest Reynolds numbers both the initial decrease and the first sudden increase are usually absent.

These results are qualitatively explainable by comparing the flow near the inlet to the flow near the leading edge of a flat plate. In order to make this comparison clearer, the results of figures 2 to 5 are replotted in figures 6 to 9 as local apparent friction coefficient against R_x. Also, figure 10 shows the results of Kirsten (reference 6) on this basis. For each R_D the pattern of points in figures 6 to 9 is the same as in figures 2 to 5 because the scales of the two sets of charts are proportional. In the representations of figures 6 to 10, however, the influence of R_D is relatively small as compared with its influence in the previous charts.

In figures 6 to 10 there are plotted the lines representing the drag coefficients for laminar and turbulent flow over a flat plate. The qualitative similarity between the pipe flow and the flat-plate flow is evident. Quantitative agreement cannot be expected because the values of f_{APP} include the effects of both shearing stress and momentum

change, whereas the drag coefficient for the flat plate represents only the shearing stress; also, the pressure gradients in the lengthwise direction are different for the two cases, and the flow in the boundary layer is planar only at the very inlet to the tube.

From figures 6 to 10 it appears that there are two regimes near the inlet to the tube and that the change from one regime to the other occurs at a value of R_x of about 5×10^5. It is notable that the change from laminar to turbulent flow for a flat plate (reference 7, pp. 139-143) also occurs at about $R_x = 5 \times 10^5$. The similarity in the slopes of the curves for the tube and the plate in both the laminar and turbulent regimes is also worthy of mention. For very high values of R_x the comparison naturally breaks down altogether, for the boundary layer in the pipe then becomes large compared to the radius, and the apparent friction coefficient becomes independent of R_x.

With the foregoing facts in mind, the following summary of events near the inlet of the tube seems reasonable. A laminar boundary layer first forms and develops in a manner comparable with that for a flat plate, and the friction coefficient decreases with increasing R_x. At a value of R_x of about 5×10^5, the boundary layer changes from laminar to turbulent, and the friction coefficient rises sharply. Subsequently the friction coefficient shows a general trend downward toward an asymptote because the rate of change of velocity profile is gradually reduced. The irregular effects which occur shortly after the change from a laminar to a turbulent boundary layer are probably the result of rather rapid adjustments of velocity profile within the boundary layer.

From the trend of the data and from the simple physical considerations just described, it appears that the local apparent friction coefficient is infinite at the inlet to the tube and that it then decreases approximately in inverse proportion to the six-tenths power of the distance from the inlet. The highest reported value of f_{APP} in the laminar inlet zone, measured at $\frac{x}{D} = 0.5$, is about 3.5 times the Kármán-Nikuradse value. The lowest measured values of f_{APP} in the laminar inlet zone are less than half the Kármán-Nikuradse value for fully developed turbulent flow.

In the transition zone immediately following the change from a laminar to a turbulent boundary layer the maximum values of f_{APP}/f_{K-N} are about 1.5, and the minimum values are about 0.8.

It is difficult to determine with precision from the results given herein the value of x/D at which inlet effects become negligible.

However, it appears that the value of f_{APP} is confined within 10 percent of the Kármán-Nikuradse value beginning at about 20 to 30 tube diameters from the tube inlet. The value of f_{APP} is confined within 5 percent of the Kármán-Nikuradse value beginning at about 40 to 60 tube diameters from the tube inlet. These x/D values are far smaller than those predicted by the laminar inlet theories of Boussinesq, Schiller, and Langhaar and are about three times as large as the value predicted by the turbulent inlet theory of Latzko (refer to section "Historical Background" under INTRODUCTION).

Integrated Friction Coefficient

For design purposes the most important quantity is the total pressure drop from the inlet to any point downstream. This value is represented by the integrated apparent friction coefficient, which in figure 3(b) is shown plotted against x/D for the water tests with tube II. Because of the cumulative nature of f_{APP}, the curves of figure 3(b) show much less variation than those of figure 3(a), particularly at high values of x/D.

In general, the integrated friction coefficient at any x/D value greater than 20 is larger than the Kármán-Nikuradse value when R_D is greater than 100,000 and is less than the Kármán-Nikuradse value when R_D is less than 100,000.

Effects of Induced Turbulence

Figures 11 and 12 show the effects of introducing turbulence artificially.

There are two possible explanations of the results of figure 11:

(a) Initial turbulence moved the point of transition from a laminar to a turbulent boundary layer forward from $R_x \cong 5 \times 10^5$ to $R_x \cong 1 \times 10^5$.

(b) Initial turbulence caused the boundary layer to be turbulent from the inlet. The trend upward of f_{APP} near the inlet makes the first explanation physically more plausible, although the data are insufficient for a definite conclusion to be drawn.

The effects of induced turbulence shown in figure 12 are not strictly comparable with the effects shown in figure 11 because in the air tests of tube IV the device for producing turbulence was inserted at the beginning of the cylindrical section of the tube. Presumably, the turbulence for tube IV was considerably greater than that for tube II.

Figure 12 shows clearly that induced turbulence may act to increase considerably the value of f_{APP} in the region which would normally be the laminar inlet zone. From the absence of a sharp transition zone it appears reasonable to conclude that in the tests with tube IV the boundary layer was turbulent over the range of x/D values in which measurements were made. The observed decrease of the apparent friction coefficient with increasing x/D, followed by a gradual trend toward a constant friction coefficient, is probably attributable chiefly to the momentum effects of the developing velocity profile.

It appears from figure 12 that a small obstruction on the wall is much more effective in tripping the boundary layer than is a screen across the entire duct. In fact, in the region where R_x is less than 5×10^5, the strip of scotch tape led to about an eightfold increase in the apparent friction coefficient, whereas the screen at the inlet cross section led to about a threefold increase in friction coefficient. Also, the scotch-tape strip acted to raise by a factor of about two the value of the apparent friction coefficient in what would normally be the turbulent zone of developing velocity distribution. The effect of the screen was not so marked in this respect and indeed is not easy to summarize from figure 12.

Laminar Inlet Zone

Langhaar (reference 4) arrived through analytical reasoning at a relation between f_{APP} and the single parameter $(x/D)/R_D$. From his table II there was deduced by calculation a series of curves of f_{APP} against R_x for constant values of R_D. These curves based on Langhaar's work have been inserted in figures 6 to 10. It is evident from these charts that in the laminar portion of the inlet zone the theoretical results based on Langhaar's work compare favorably with the measured results. The comparison is particularly impressive for the water tests of tube II, which, for various reasons, are probably the most reliable tests of those reported herein.

In examining the results shown in figure 9 for the air tests with tube IV, it should be borne in mind that the apparent scattering in the laminar zone was not physically present but is artificially introduced because of the errors associated with small spacing between pressure taps. Viewed in this light, the results of figure 9 support Langhaar's theory almost as well as do the results of figures 6 to 8.

More precise agreement between the measured results and the results based on Langhaar can scarcely be expected, since there are several inconsistent sources of divergence to be expected, among which are:

(a) Langhaar's theory is based on a uniform velocity profile at $x = 0$. This condition was only approximated in the experiments.

(b) Langhaar's theory is based on uniform pressure over each cross section. The slight deviations from this, taken together with the small pressure differences between taps, might be a cause of disagreement.

(c) The theory neglects any boundary layer which forms on the bellmouth entry.

In the light of these remarks it seems fair to conclude that the theory of Langhaar predicts apparent friction coefficients in the laminar inlet zone with satisfactory accuracy.

Before leaving the subject of the laminar inlet zone, it is of interest to compare the theoretical results of Langhaar with those of Schiller and of Atkinson and Goldstein. Figure 13 shows that for values of the parameter $(x/D)/R_D$ greater than 0.0005, the results of Schiller agree well with those of Langhaar. Atkinson and Goldstein disclaim accuracy for their results when $(x/D)/R_D$ is less than 0.0075. Figure 13, however, shows their results and those of Langhaar to be still within about 7 percent at this value of $(x/D)/R_D$. It is noteworthy that the agreement among the various theories that consider rate of development of the velocity profile as to the total pressure drop from the inlet is much better than the agreement as to velocity profile. This is not surprising in view of the remarkable success of the Kármán momentum equations for prediction of drag, a success based largely on the insensitivity of the change in momentum flux to the type of velocity profile initially assumed.

In order to illustrate the importance of the developing velocity profile, figure 13 shows also the results based on Poiseuille flow, that is, laminar flow with a parabolic velocity profile present from the inlet. For a tube length and Reynolds number corresponding to $\frac{(x/D)}{R_D} = 0.0005$, the total pressure drop predicted by Langhaar is 10 times as great as that corresponding to Poiseuille flow. At $\frac{(x/D)}{R_D} = 0.1$, which is beyond the value at which the theories predict a nearly fully developed velocity profile, the total pressure drop based on Poiseuille flow (considering a parabolic velocity profile) is about 20 percent less than that predicted by Langhaar. When the length of tube is infinite, or more strictly, when $(x/D)/R_D$ is very large, the inlet effects are relatively insignificant, so that the curve of Langhaar approaches that of Poiseuille asymptotically.

Comparison of Measured Results Obtained with Different Tubes

In comparing the measured results obtained with tubes I, II, III, and IV, the representations of figures 2 to 5 are almost useless because the effect of R_D is too strong on these charts. A better comparison is afforded by figures 6 to 9, for which the results of Langhaar may be used as reference lines to aid the comparison. Taken as a whole, the agreement among the results for the four tubes seems quite satisfactory. In the next section it can be seen that the agreement among tubes I, II, and III as regards the developed friction coefficient is very satisfactory.

The differences among the results shown in figures 6 to 9 may be ascribed largely to the different type of entry used with each tube. Not only does the shape of the entry affect the velocity profile at the inlet to the tube proper, but it also has a great influence on the thickness of the boundary layer at the inlet to the tube.

From figures 6 and 7 it appears that the change from the long-pipe entry of figure 1(b) to the stilling-chamber entry of figure 1(e) acted to delay the point of transition to a turbulent boundary layer from $R_x \cong 2 \times 10^5$ to $R_x \cong 4 \times 10^5$. This is doubtless a result of the lesser initial turbulence present when the stilling chamber was used.

The few results reported by Kirsten, figure 10, fit well with the results of the present investigation.

Developed Friction Coefficient

Tubes I and II were so long that it was possible to obtain data in a region where the variations in f_{APP} were within the limits of experimental accuracy. The values of f_{APP} thus obtained are called the developed friction coefficient f_{DEV}. Presumably, the changes in velocity profile were negligible over the range herein considered.

Figure 14 shows the measured values of f_{DEV} plotted against R_D, with the curve of Kármán-Nikuradse inserted for comparison. The measured values are consistently higher than the Kármán-Nikuradse values for the same R_D. Considering tubes I and II only, the average value of the developed friction coefficient is 1.3 percent higher than the value of the Kármán-Nikuradse coefficient at the same Reynolds number. The precision of the measured data may be judged from the fact that the average deviation from a smooth curve through the measured values of f_{DEV} is about one-third of 1 percent. Whether the consistent departure of the measured results from the Kármán-Nikuradse values is the result of systematic errors in either the former or the latter cannot be ascertained without further data.

Figure 14 shows also the values of f_{DEV} for tube III. It is open to question whether these results should properly be considered as the developed friction coefficient, since the two x/D values over which f_{DEV} was measured were $\frac{x}{D} = 44$ and $\frac{x}{D} = 126$. The departure of the developed friction coefficient from the Kármán-Nikuradse value by as much as 6 percent is doubtless the consequence of small changes in velocity profile. This supposition is lent added weight by the qualitative agreement between the way in which f_{DEV}/f_{K-N} varies with R_D and the fact that $(x/D)/R_D$ appears to be an approximate parameter for representing the relative importance of changes in velocity distribution. In other words, for a fixed value of x/D, large values of R_D indicate large effects due to a changing velocity profile, and vice versa, which seems to be in agreement with the results for tube III shown in figure 14.

Application to Discharge Coefficients for Rounded-Entrance Flow Nozzles

Nozzles for flow measurement usually comprise a bellmouth entry with an elliptical- or circular-arc cross section followed by a short cylindrical section. The downstream pressure tap is commonly placed at 1/2 throat diameter downstream from the inlet to the cylindrical section but may in some designs be at a different location.

Departures of the discharge coefficient from unity are caused by friction and by a developing velocity profile. Both these effects on the pressure drop are taken into account by the integrated apparent friction coefficient. In the appendix, it is shown that the discharge coefficient may be expressed approximately by the formula

$$c_w = \sqrt{\frac{1}{1 + 4\bar{f}_{APP}\,(x/D)}}$$

where x/D is the length-diameter ratio of the short cylindrical section of the flow nozzle. If friction in the bellmouth entry is appreciable, the foregoing formula is still approximately applicable in terms of an effective x/D for the combined bellmouth and cylindrical section. A crude method for evaluating the effective x/D of the bellmouth is given in the appendix.

The results of the present investigation indicate that up to $R_x \cong 5 \times 10^5$ the boundary layer is laminar and that the theory of Langhaar fits the experimental data with good accuracy. The curve of Langhaar in

figure 13 was accordingly employed as described in the appendix for computing theoretically the discharge coefficients for values of x/D corresponding to standard flow nozzles and over a range of R_D values which in each case would insure a laminar boundary layer up to the downstream pressure tap.

Figure 15(a) shows a comparison between the computed discharge coefficients and the average of the measured discharge coefficients reported in references 13 and 14. The nozzles referred to in references 13 and 14 had cylindrical portions with $\frac{x}{D} = 0.50$ and effective x/D values for the entire nozzle of very nearly unity. In figure 15(a) the computed curves are therefore given for values of x/D of both 0.5 and 1.0. The agreement between the computed and measured discharge coefficients is remarkable when it is considered that the curve for the effective ratio of $\frac{x}{D} = 1.0$ fits the average curve of measured coefficients within the accuracy to which the latter were measured.

Figure 15(b) shows a comparison between the computed discharge coefficient and the average curve based on measurements at low Reynolds numbers by Downie Smith and Steele (reference 15). The nozzle used by Downie Smith and Steele had a cylindrical section 2.5 diameters long and a bellmouth entry with an effective x/D of about 0.5. In figure 15(b) the computed curves are therefore given for values of x/D of both 2.5 and 3.0. The effect of the bellmouth is evidently much less important in this case than in the case of the A.S.M.E. flow nozzle. Discrepancies among the two computed curves and the one experimental curve of figure 15(b) are within the experimental precision of the data of Downie Smith and Steele.

It seems plain from the comparisons of figures 15(a) and 15(b) that the method presented herein for the prediction of discharge coefficients is well founded in its physical concepts. The method should find use for estimating the way in which the discharge coefficient depends on the location of the downstream pressure tap of rounded-entrance flow nozzles. The analysis also explains much of the disagreement among the experimentally measured discharge coefficients for flow nozzles of slightly different design.

CONCLUSIONS

From an experimental study of friction coefficients near the inlet of smooth, round tubes with bellmouth entrances, the following conclusions can be drawn:

1. Near the inlet to a tube with a bellmouth entrance the boundary layer is at first laminar and subsequently becomes turbulent at a value

of Reynolds number (based on tube inlet) of about 5×10^5, which is about the same as the corresponding value for a flat plate. The apparent friction coefficient in the laminar inlet zone varies approximately inversely with the 0.6 power of the distance from the inlet. A sharp rise in apparent friction coefficient accompanies the change from a laminar to a turbulent boundary layer. Near the beginning of the turbulent inlet zone there are rapid and irregular changes in the local apparent friction coefficient which are probably the result of rapid adjustments of velocity profile within the boundary layer.

2. The reported values of the local apparent friction coefficient f_{APP} vary in the laminar inlet zone from 3.5 to 0.5 times the Kármán-Nikuradse coefficient f_{K-N} for fully developed turbulent flow. Very near the inlet it is probable that f_{APP} is almost infinite compared with f_{K-N}. In the turbulent inlet zone the reported values of f_{APP} range from 1.05 to 0.8 times f_{K-N}. The value of f_{APP} remains within 5 percent of f_{K-N} beginning at about 40 to 60 diameters from the tube inlet.

3. The integrated apparent friction coefficient $\bar{f}_{APP}$, which is a measure of the total pressure drop from the inlet, ranges from 0.9 to 1.25 times the value of f_{K-N} for the tubes which are 20 diameters in length. Over a range of Reynolds number from 40,000 to 250,000 about 80 tube diameters are required for $\bar{f}_{APP}$ to remain within 5 percent of $\bar{f}_{K-N}$. In general, $\bar{f}_{APP}/f_{K-N}$ is less than unity when the Reynolds number (based on tube diameter) is less than 100,000 and is greater than unity for Reynolds numbers greater than 100,000.

4. Inducing turbulence artificially acts either to move forward the point of transition from a laminar to a turbulent boundary layer or to eliminate the laminar boundary layer altogether. A strip of scotch tape on the wall was much more effective in tripping the boundary layer than was a wire screen over the entire cross section. In the laminar inlet zone the scotch tape led to about an eightfold increase in f_{APP}, whereas the wire screen caused about a threefold increase.

5. The measured values of f_{APP} in the laminar inlet zone support the laminar inlet theory of Langhaar. The integrated apparent friction coefficients given by the laminar inlet theories of Langhaar, Schiller, and Atkinson and Goldstein are in good agreement despite the wide divergences in predicted velocity profiles.

6. The measured results obtained with four different tubes and with air and water used as the flowing medium were in satisfactory agreement.

Differences in the approach section and in the bellmouth entry were probably accountable for the observed differences between the results with the four tubes. The data of Kirsten for air flowing in smooth tubes are in good agreement with the present results.

7. The friction coefficient for developed flow was about 1.3 percent higher than the Kármán-Nikuradse coefficient at the same Reynolds number and displayed an average scattering about a mean curve of only one-third of 1 percent. The source of the systematic disagreement of 1.3 percent between the measured values of the developed friction coefficient and the Kármán-Nikuradse value is not known.

8. A method based on the experimental results of this investigation was presented for estimating the discharge coefficient for rounded-entrance flow nozzles. Discharge coefficients computed on this basis were found to be in excellent agreement with published information on flow nozzles.

Massachusetts Institute of Technology
Cambridge, Mass., July 29, 1947

APPENDIX

APPROXIMATE RELATION BETWEEN DISCHARGE COEFFICIENTS OF FLOW NOZZLES AND FRICTION COEFFICIENTS IN INLET ZONE

Consider a bellmouth entry leading from a large stilling chamber to a short cylindrical tube of diameter D and length x. Let the pressures in the stilling chamber, the inlet to the tube, and the station x be denoted by p_o, p_1, and p_2, respectively. The flow is considered imcompressible.

As a first approximation the effects of friction in the bellmouth will be neglected. In that case,

$$p_o - p_1 = \frac{\rho}{2} V^2 \tag{8}$$

For the cylindrical tube, from equation (5),

$$p_1 - p_2 = 4\bar{f}_{APP} \frac{x}{D} \frac{\rho}{2} V^2 \tag{9}$$

Adding equations (8) and (9),

$$p_o - p_2 = \frac{\rho}{2} V^2 \left[1 + 4\bar{f}_{APP} \left(\frac{x}{D}\right)\right] \tag{10}$$

The flow coefficient is defined by

$$c_w = w/A\rho \sqrt{2\left(p_o - p_2\right)/\rho} \tag{11}$$

Upon noting that $w = \rho AV$ and combining this with equations (10) and (11), there is finally obtained

$$c_w = \frac{1}{\sqrt{1 + 4\bar{f}_{APP} (x/D)}} \tag{12}$$

If the boundary layer up to station x is laminar, the experimental data reported herein indicate that the curve marked "Langhaar" in figure 13 may be used for finding the value of $4\bar{f}_{APP}(x/D)$ corresponding to the given value of x/D and any arbitrary value of R_D. Using equation (12), c_w may then be found as a function of R_D, as illustrated by figure 15.

The frictional effects in the bellmouth entry may on occasion not be negligible. There seems to be no simple way of taking these effects into account with accuracy. However, the order of magnitude of the effects can probably be found by treating the flow in the bellmouth as one-dimensional and by assuming that neither the curvature of the streamlines nor the pressure gradient alters the friction coefficient. The procedure then involves the computation of an effective x/D for the bellmouth which is then added to the x/D of the cylindrical tube to give the effective x/D of the entire nozzle.

In finding the effective x/D of the bellmouth, it is first noted that

$$dp = 4f_{APP} \frac{dx}{D_i} \frac{\rho}{2} V_i^2 = 4f_{APP}\, d(x/D)\, \frac{\rho}{2} V^2 \left(\frac{V_i}{V}\right)^2 \left(\frac{D}{D_i}\right)$$

where the subscript i refers to conditions in the entry section.

Also, since

$$\frac{V_i}{V} = \left(\frac{D}{D_i}\right)^2$$

it follows that

$$\Delta\left(\frac{x}{D}\right)_{effective} = \int \left(\frac{D}{D_i}\right)^5 d\left(\frac{x}{D}\right) \qquad (13)$$

where the limits of integration are from the beginning to the end of the bellmouth entry. As an example, for a bellmouth made up of a circular-arc cross section with an arc radius of D, the effective x/D of the bellmouth is about 0.4.

REFERENCES

1. Boussinesq, J.: Hydrodynamique Comp. Rend., t. 110, 1890, pp. 1160, 1238; t. 113, 1891, pp. 9, 49.

2. Schiller, L.: Die Entwicklung der laminaren Geschwindigkeitsverteilung und ihre Bedeutung für Zähigkeitsmessungen. Z.f.a.M.M., Bd. 2, Heft 2, pp. 96-106.

3. Fluid Motion Panel of the Aeronautical Research Committee and Others: Modern Developments in Fluid Dynamics. Vol. I, S. Goldstein, ed., The Clarendon Press (Oxford), 1938, pp. 304-308.

4. Langhaar, Henry L.: Steady Flow in the Transition Length of a Straight Tube. Jour. Appl. Mech., vol. 9, no. 2, 1942, pp. A-55 - A-58.

5. Latzko, H.: Der Wärmeübergang an einen turbulenten Flüssigkeits-oder Gasstrom. Z.f.a.M.M., Bd. 1, Heft 4, 1921, pp. 268-290.

6. Kirsten, H.: Experimentalle Untersuchung der Entwicklung der Geschwindigkeitsverteilung bei der turbulenten Rohrstromungen. Doctoral Dissertation, Leipzig, 1927 (available at Harvard Library).

7. Prandtl, L., and Tietjens, O. G.: Applied Hydro- and Aeromechanics. First ed., McGraw-Hill Book Co., Inc., 1934, pp. 27, 139-143.

8. Brooks, W. B., Craft, J. P., Jr., and Montrello, J.: Friction Factor for Turbulent Flow in Transition Region for Straight Pipe. Thesis, Dept. of Marine Eng., M.I.T., Cambridge, Mass., 1943.

9. Smith, R. D.: Friction Factors for Turbulent Flow in Transition Region for Straight Tubes. Thesis, Dept. of Mech. Eng., M.I.T., Cambridge, Mass., 1947.

10. Anon.: Report of a Joint Committee on Orifice Coefficients of the American Gas Association and the A.S.M.E., New York, 1936.

11. Nikuradse, J.: Gesetzmässigkeiten der turbulenten Strömung in glatten Rohren. VDI, Forschungsheft 356, 1932.

12. Von Kármán, Th.: Turbulence and Skin Friction. Jour. Aero. Sci., vol. 1, no. 1, Jan. 1934, pp. 1-20.

13. A. S. M. E. Power Test Codes: Information on Instruments and Apparatus. Pt. 5, Measurement of Quantity of Materials; ch. 4, Flow Measurement by Means of Standardized Nozzles and Orifice Plates, 1940, pp. 29, 40.

14. Buckland, B. O.: Fluid-Meter Nozzles. Trans. A. S. M. E., vol. 56, no. 11, Nov. 1934, pp. 827-832.

15. Downie Smith, J. F., and Steele, Sydney: Rounded-Approach Orifices. Mech. Eng., vol. 57, no. 12, Dec. 1935, pp. 760, 780.

TABLE I

LOCATION AND SIZE OF PRESSURE TAPS

[x, distance from tube inlet (see fig. 1(c)), in.; D, internal diameter of tube (see fig. 1(c)), in.; d, diameter of pressure tap, in.]

	Tubes I and II D = 0.373			Tube III D = 0.735			Tube IV D = 4.000		
Tap	x	x/D	d	x	x/D	d	x	x/D	d
1	0.37	1.00	0.020	0.38	0.51	[a]0.020	1.00	0.25	0.040
2	.93	3.07	.020	1.13	1.53	[a].020	3.00	.75	.040
3	1.53	5.04	.020	1.88	2.55	[a].020	5.00	1.25	.040
4	2.18	7.18	.020	2.63	3.57	[a].020	9.00	2.25	.040
5	3.39	11.20	.020	4.13	5.61	.040	13.00	3.25	.040
6	4.61	15.22	.020	5.63	7.65	.040	17.00	4.25	.040
7	7.05	23.26	.020	8.63	11.73	.040	21.00	5.25	.040
8	9.49	31.31	.020	11.68	15.89	.040	25.00	6.25	.040
9	11.92	39.35	.020	14.63	19.89	.040	29.00	7.25	.040
10	16.80	55.44	.020	20.63	28.05	.040	33.00	8.25	.040
11	21.67	71.52	.020	26.63	36.21	.040	37.00	9.25	.040
12	31.42	103.69	.020	32.63	44.37	.040	41.00	10.25	.040
13	41.17	135.86	.020	44.63	60.69	.040	49.00	12.25	.040
14	50.91	168.03	.020	56.63	77.01	.040	57.00	14.25	.040
15	60.66	200.20	.020	68.63	93.33	.040	65.00	16.25	.040
16	88.54	237.38	.020	80.63	109.65	.040	73.00	18.25	.040
17	98.68	264.55	.020	92.63	125.97	.040	81.00	20.25	.040
18	107.76	288.67	.020	104.63	144.29	.040	89.00	22.25	.040
19							97.00	24.25	.040

NACA

[a]Four taps were spaced equally around the circumference at each of these stations.

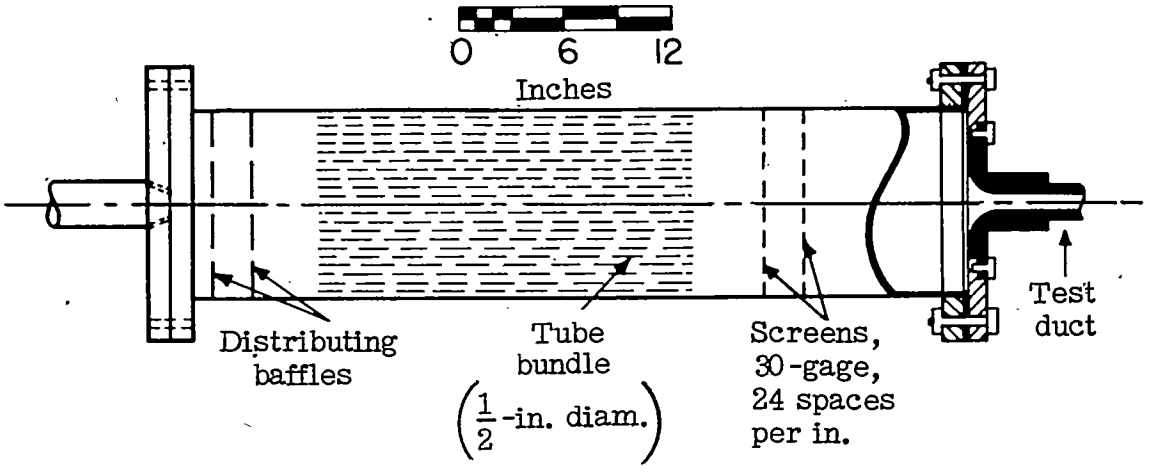

(a) Calming chamber used with tubes II and III. Distributing baffles were drilled so as to provide uniform flow over cross section. Honeycomb section was formed by a solid bank of thin brass tubes of $\frac{1}{2}$-inch diameter. Brass screening, 24-mesh, 30-gage, was used for removing turbulence.

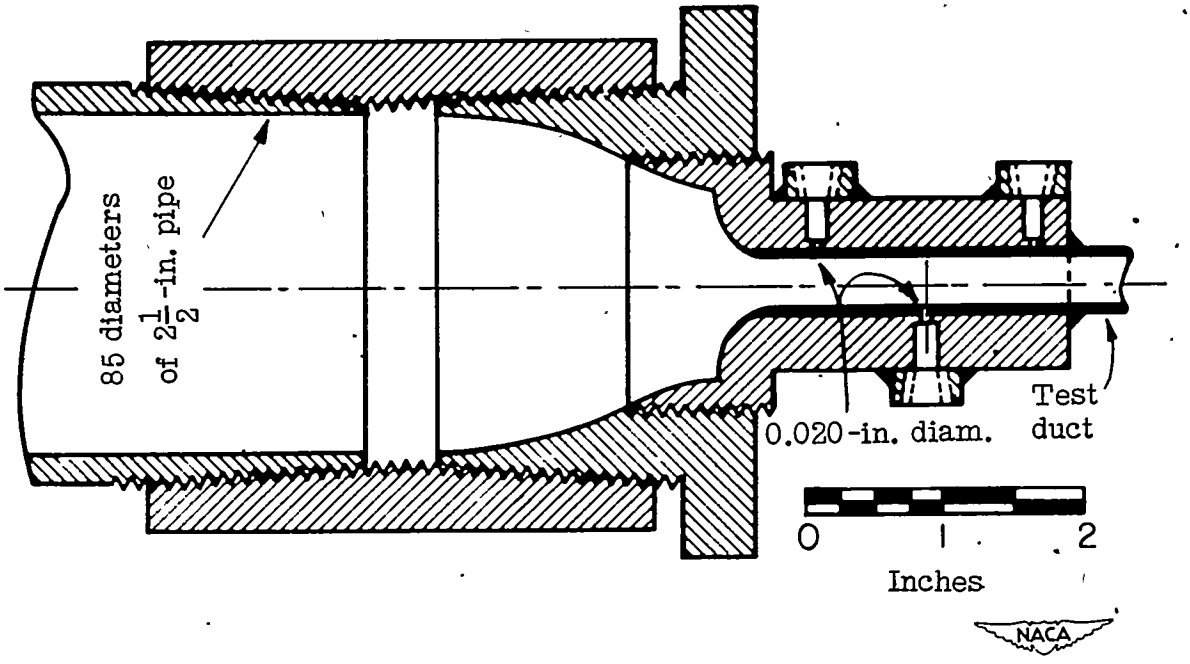

(b) Inlet to tube I, used for water tests.

Figure 1.- Test apparatus.

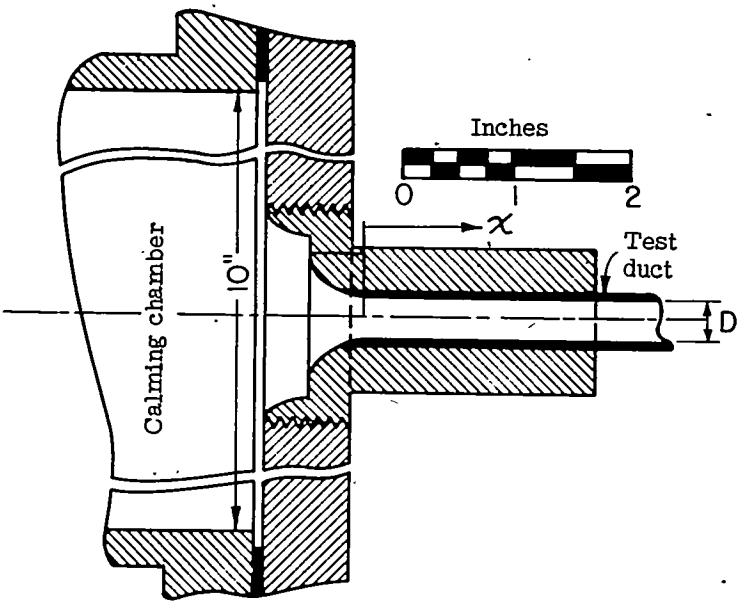

(c) Inlet to tube II, used for water tests. The same test pipe was used for tubes I and II, the sole difference being in the approach to the test section. Bellmouth entry was in cross section a circular arc with a radius of 3/8 inch.

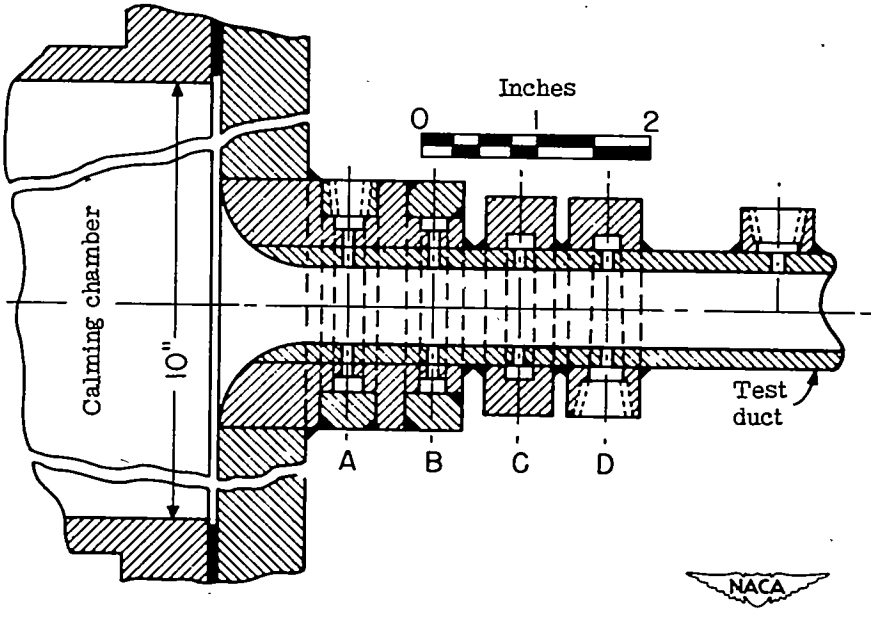

(d) Inlet to tube III, used for water tests. At stations A, B, C, and D there were four pressure taps of 0.020-inch diameter connected by a piezometer ring. The taps of stations A, B, C, and D were displaced from each other by an angle of 45° looking along axis of tube. Bellmouth entry was in cross section a circular arc with a radius of 3/4 inch.

Figure 1.- Continued.

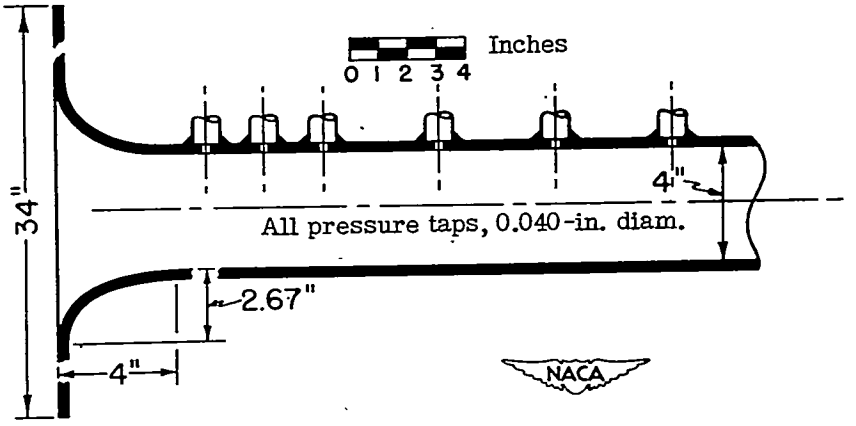

(e) Tube IV, used for air tests.

Figure 1.- Concluded.

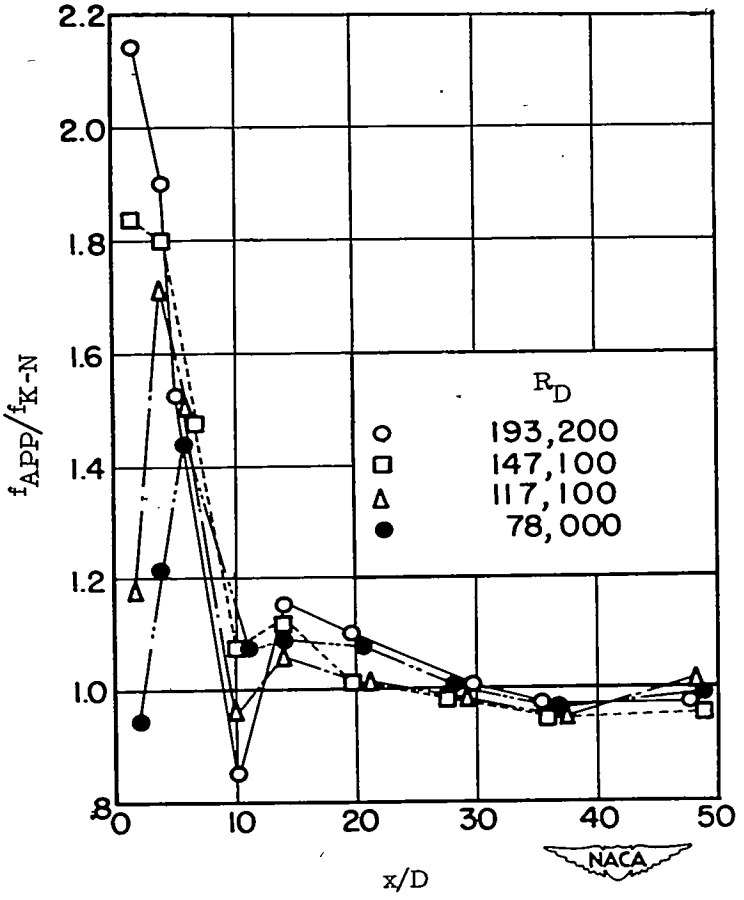

Figure 2.- Results for tube I (water tests). Ratio of local apparent friction coefficient to Kármán-Nikuradse friction coefficient against ratio of distance from inlet of duct to diameter of duct for constant values of Reynolds number based on diameter.

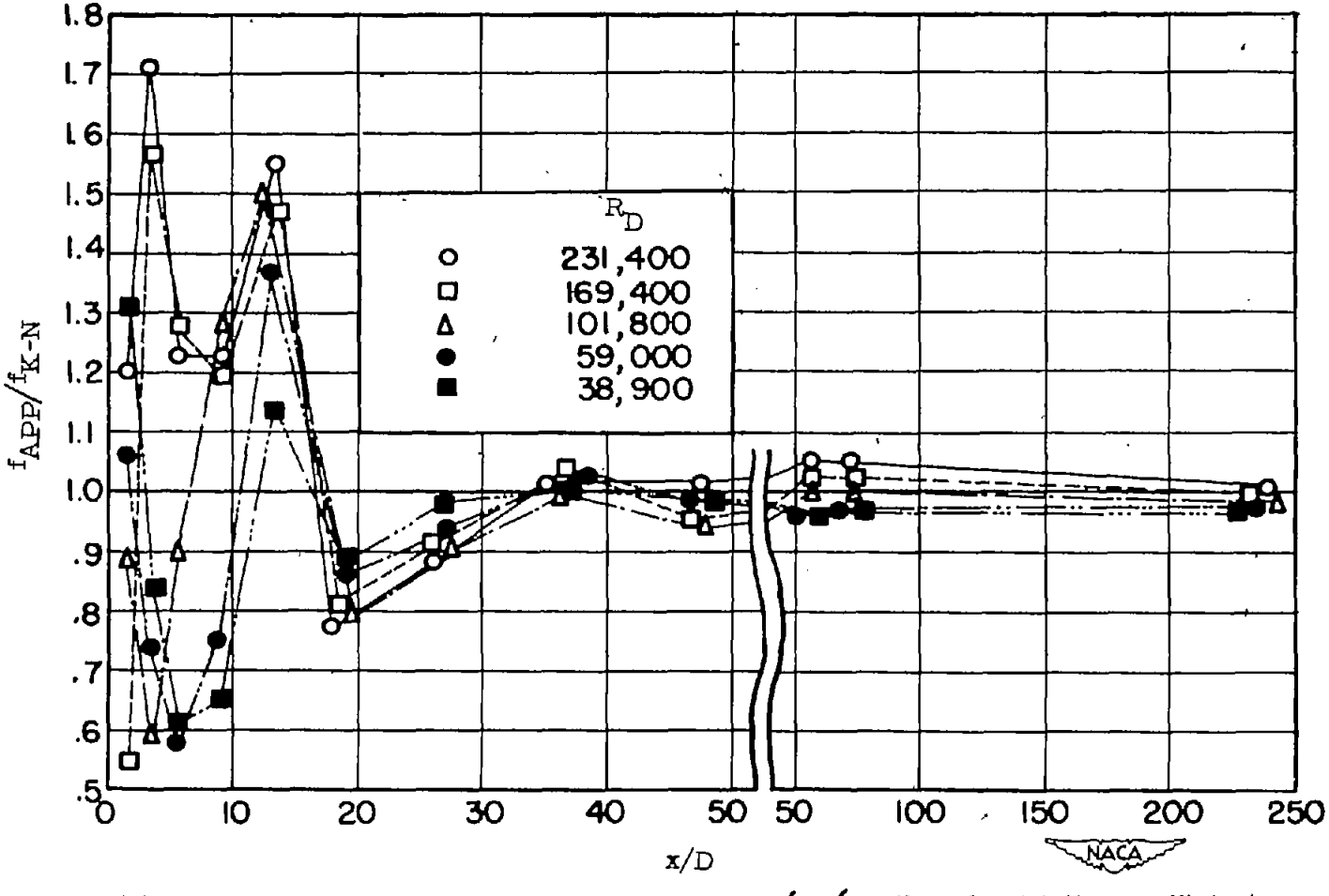

(a) Ratio of local apparent friction coefficient to Kármán-Nikuradse friction coefficient against ratio of distance from inlet of duct to diameter of duct for constant values of Reynolds number based on diameter.

Figure 3.- Results for tube II (water test).

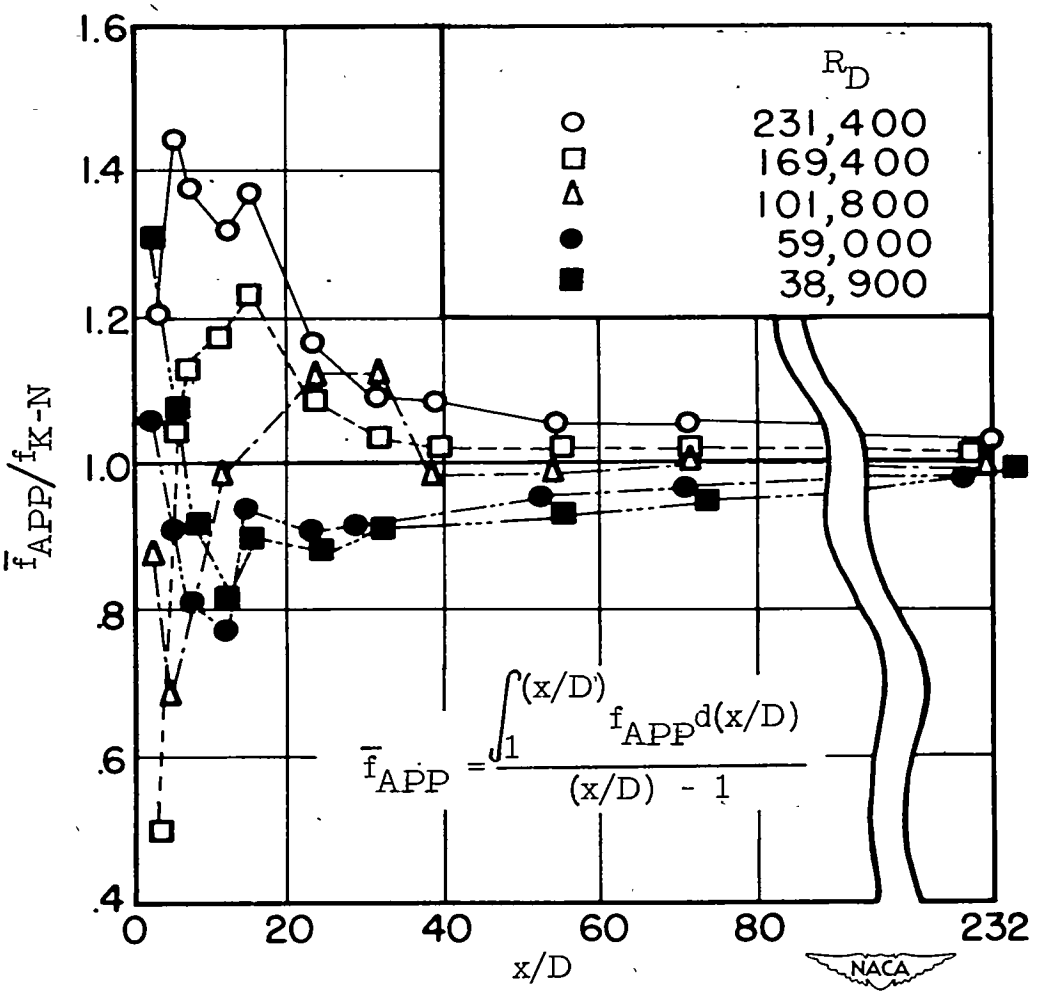

(b) Ratio of integrated apparent friction coefficient to Kármán-Nikuradse friction coefficient against ratio of distance from inlet of duct to diameter of duct for constant values of Reynolds number based on diameter.

Figure 3.- Concluded.

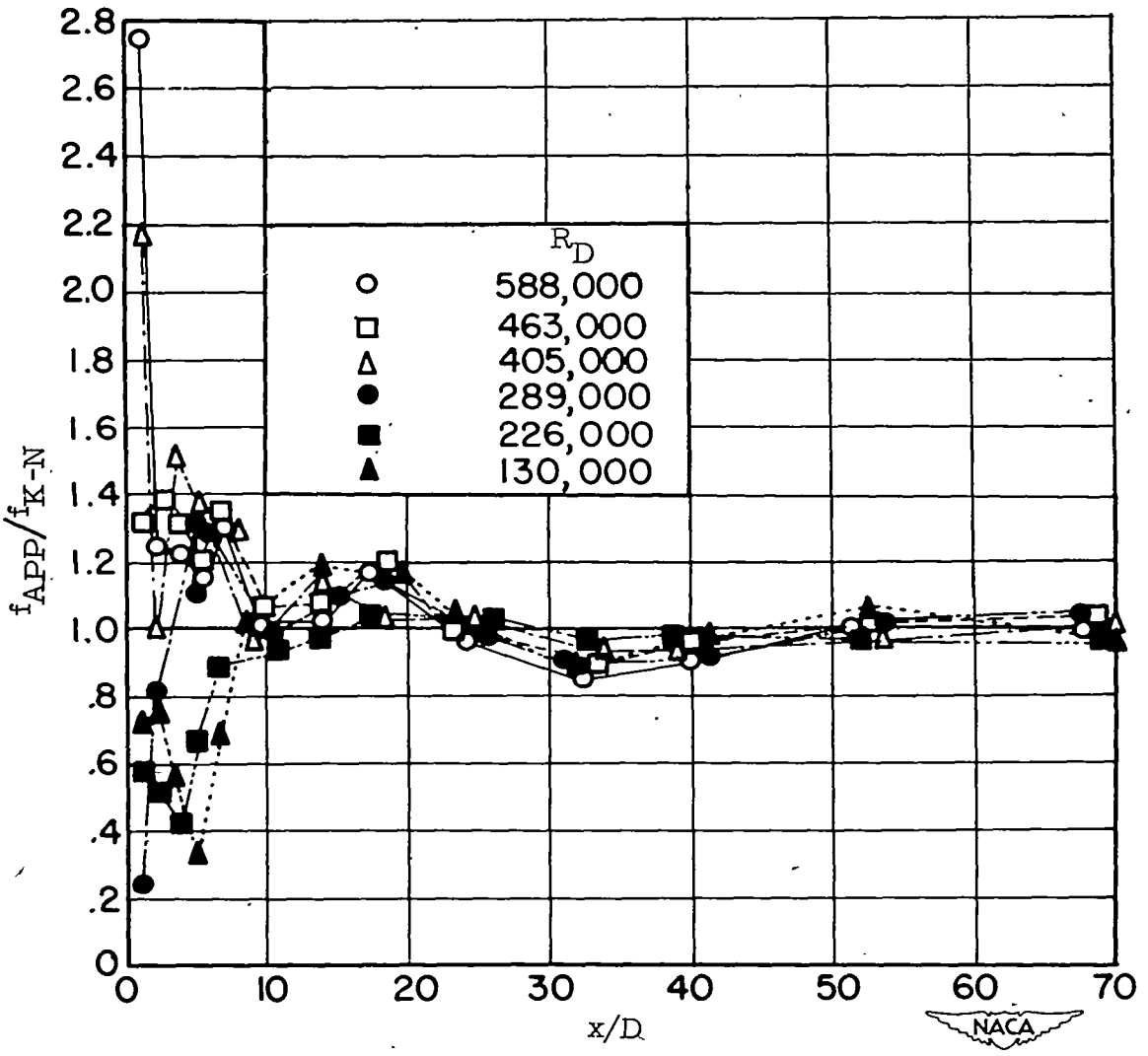

Figure 4.- Results for tube III (water tests). Ratio of local apparent friction coefficient to Kármán-Nikuradse friction coefficient against ratio of distance from inlet of duct to diameter of duct for constant values of Reynolds number based on diameter.

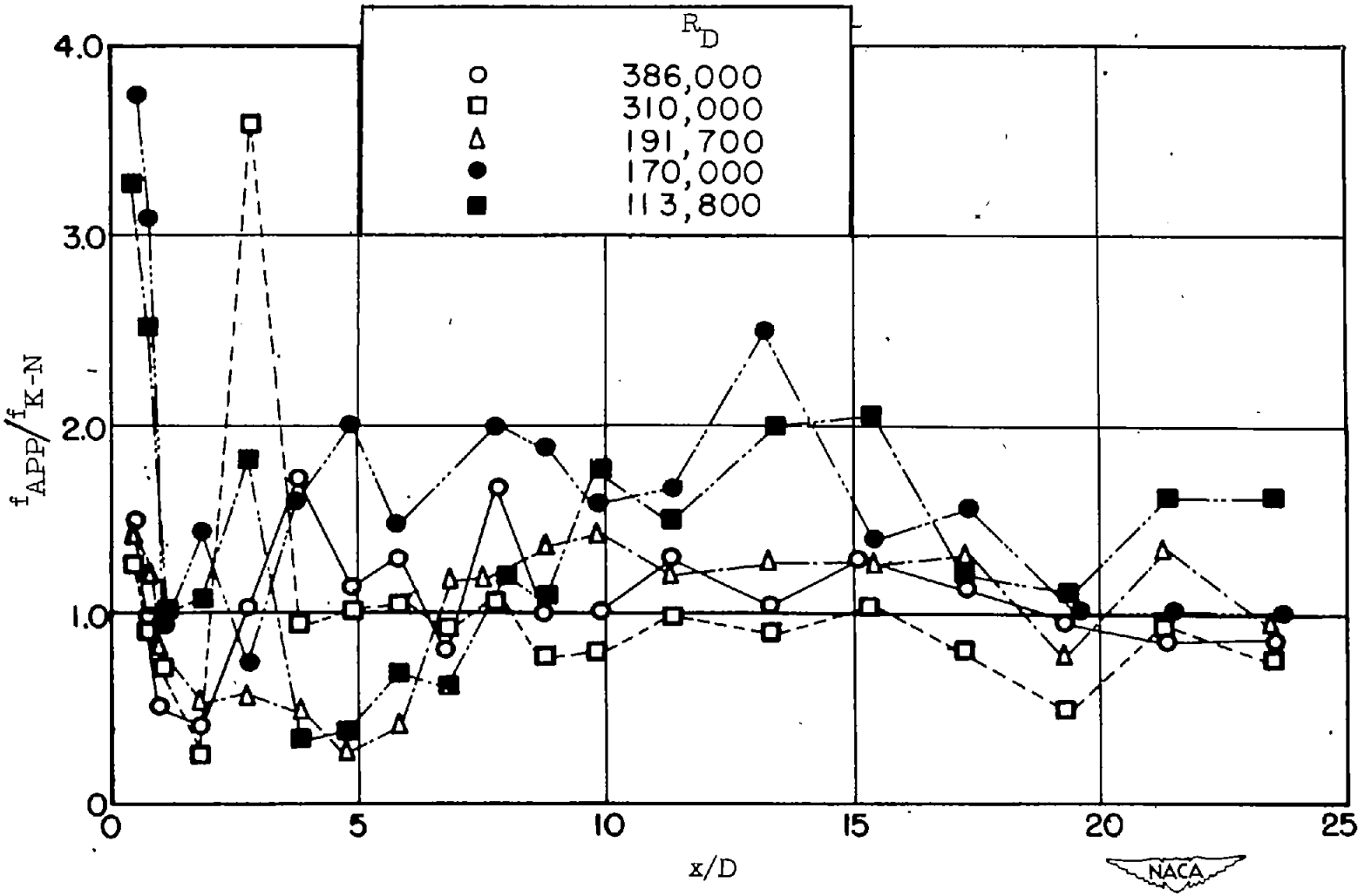

Figure 6.- Results for tube IV (air tests). Ratio of local apparent friction coefficient to Kármán-Nikuradse friction coefficient against ratio of distance from inlet of duct to diameter of duct for constant values of Reynolds number based on diameter.

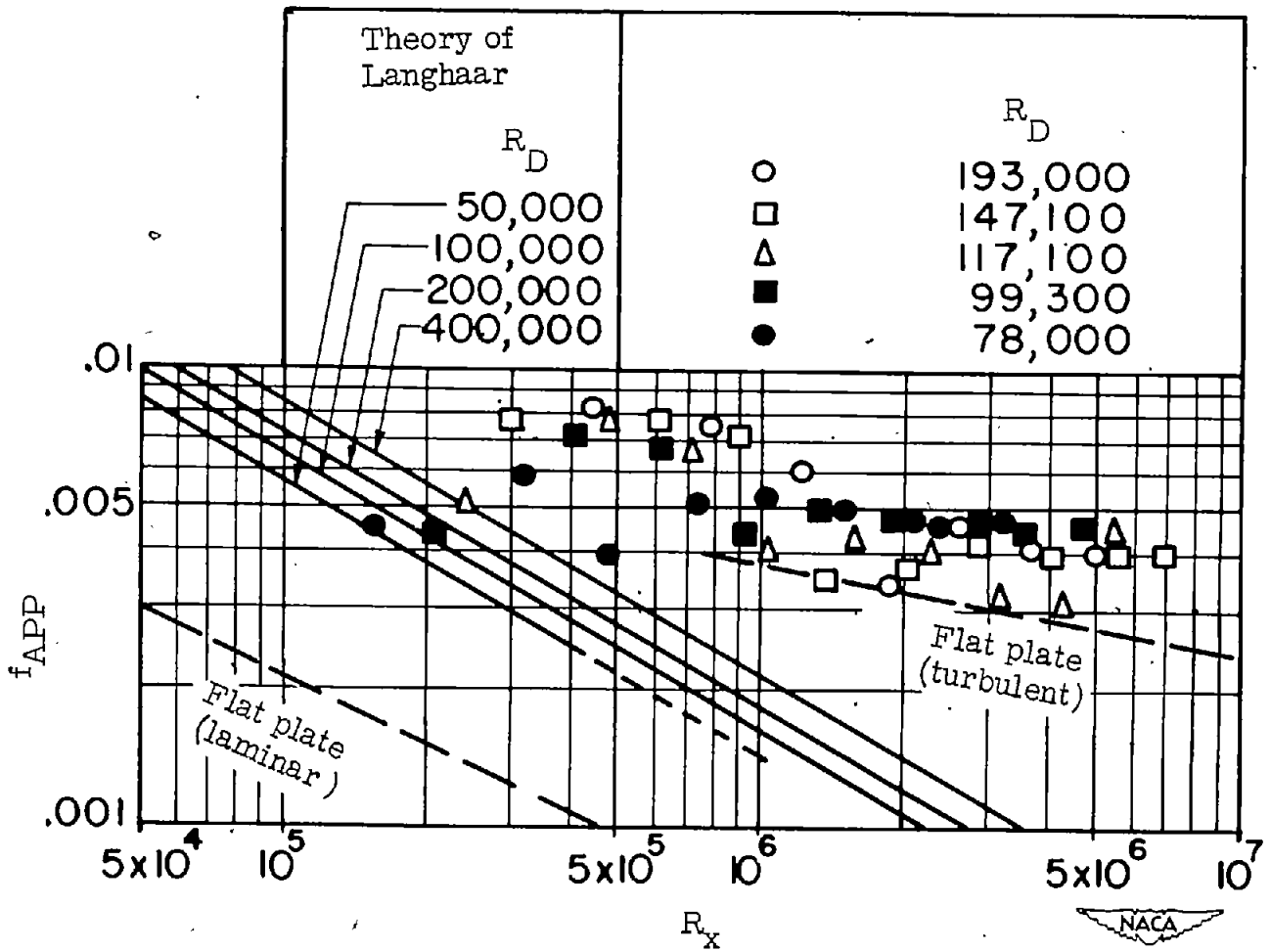

Figure 6.- Results for tube I (water tests). Local apparent friction coefficient against Reynolds number based on distance from inlet for constant values of Reynolds number based on diameter. Comparison with theoretical results of Langhaar for laminar flow. Comparison with flat-plate theory and experiment.

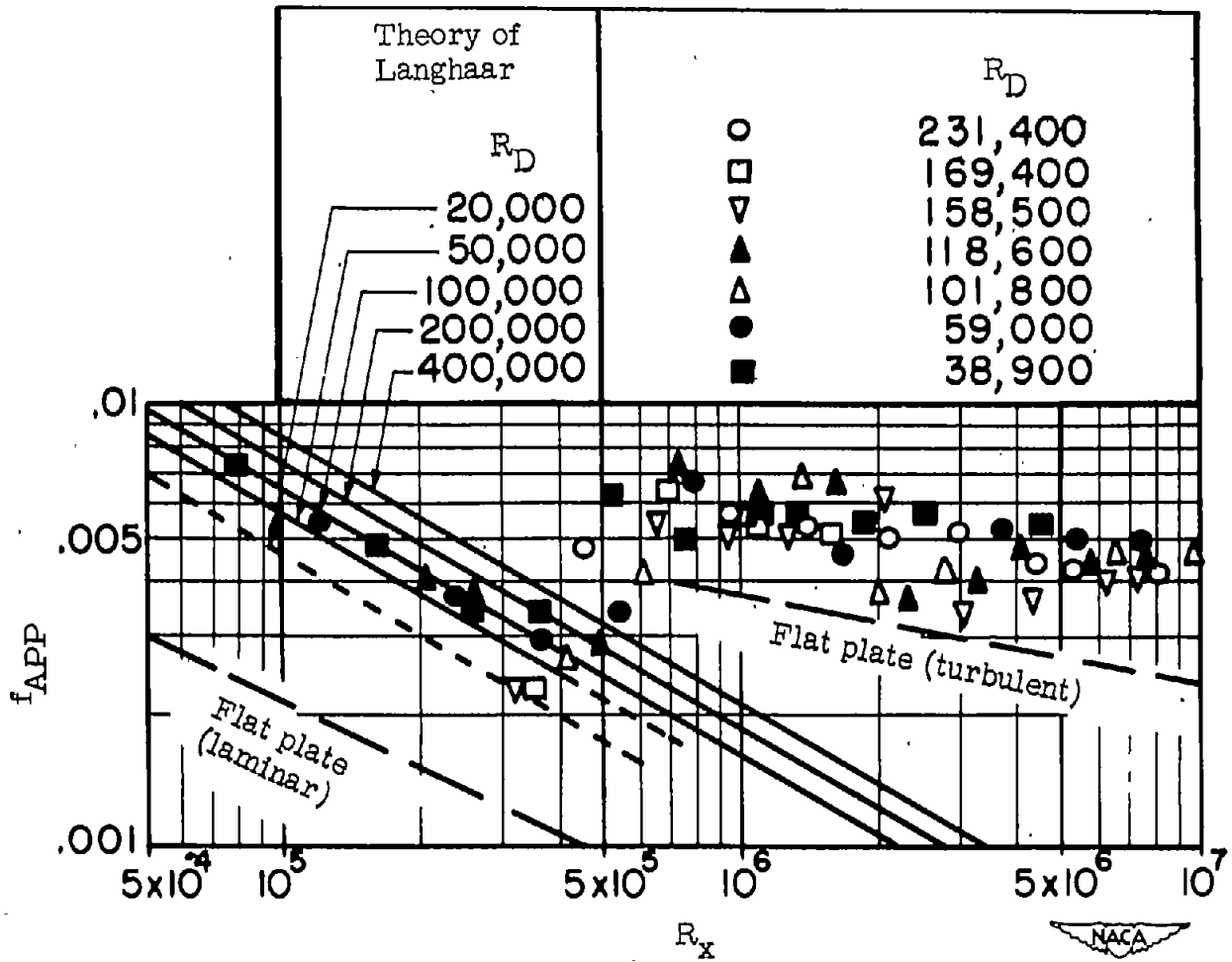

Figure 7.- Results for tube II (water tests). Local apparent friction coefficient against Reynolds number based on distance from inlet for constant values of Reynolds number based on diameter. Comparison with theoretical results of Langhaar for laminar flow. Comparison with flat-plate theory and experiment.

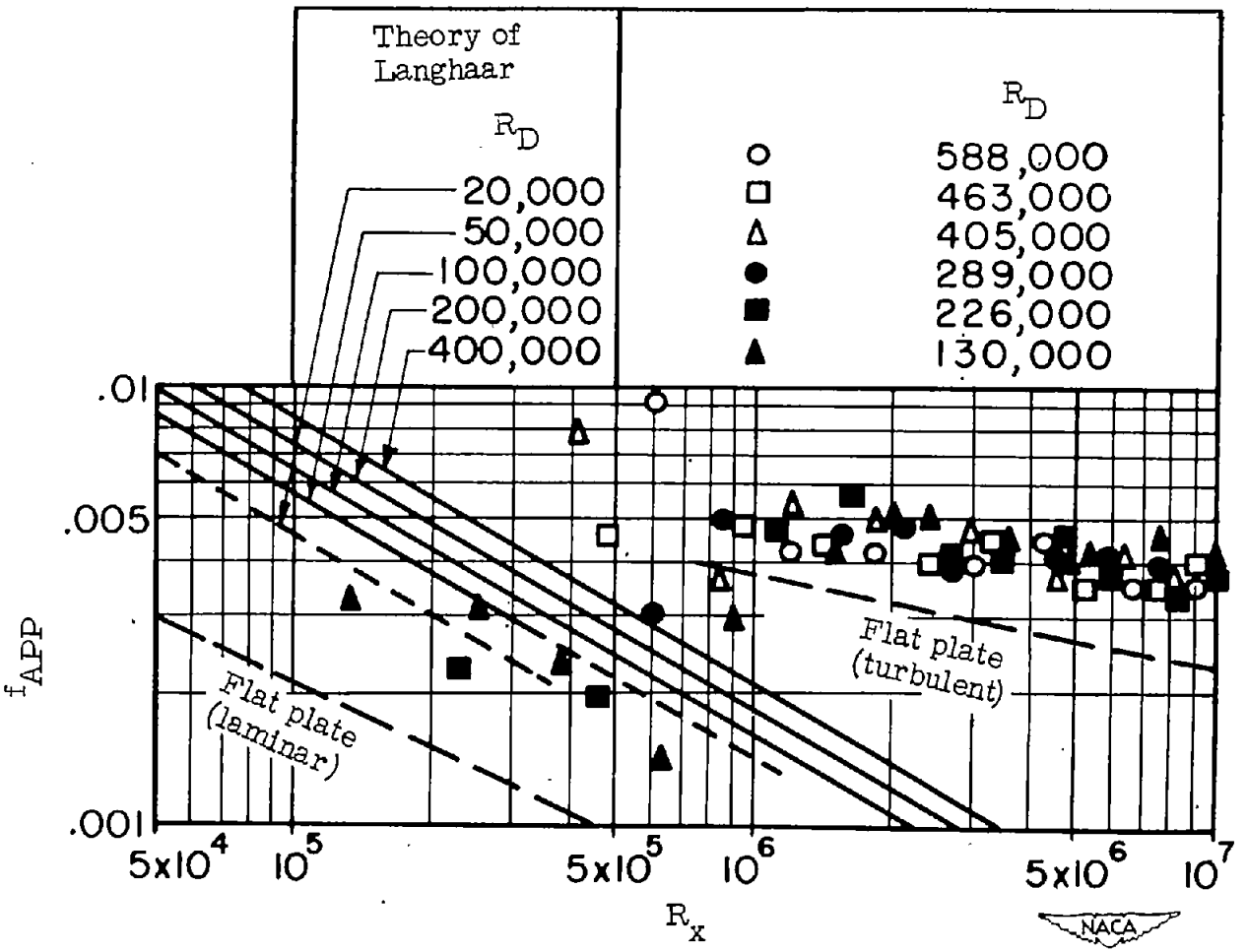

Figure 8.- Results for tube III (water tests). Local apparent friction coefficient against Reynolds number based on distance from inlet for constant values of Reynolds number based on diameter. Comparison with theoretical results of Langhaar for laminar flow. Comparison with flat-plate theory and experiment.

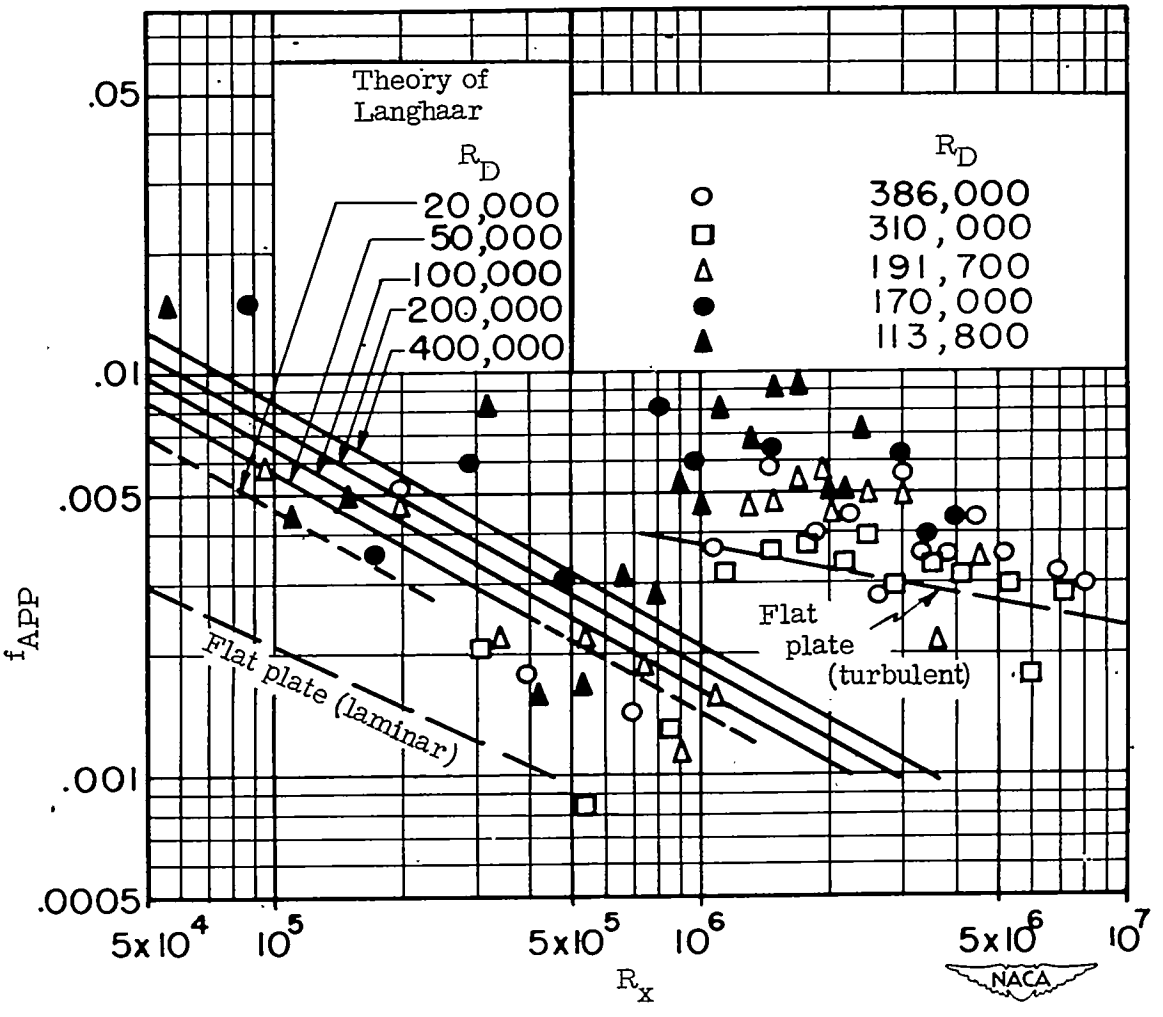

Figure 9.- Results for tube IV (air tests). Local apparent friction coefficient against Reynolds number based on distance from inlet for constant values of Reynolds number based on diameter. Comparison with theoretical results of Langhaar for laminar flow. Comparison with flat-plate theory and experiment.

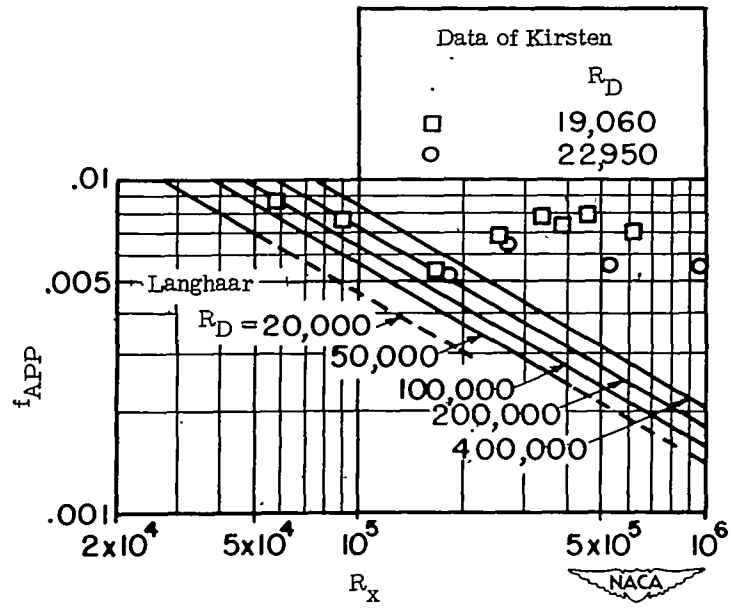

Figure 10.- Results based on Kirsten's tests with air. Local apparent friction coefficient against Reynolds number based on distance from inlet for constant values of Reynolds number based on diameter. Comparison with theoretical results of Langhaar for laminar flow.

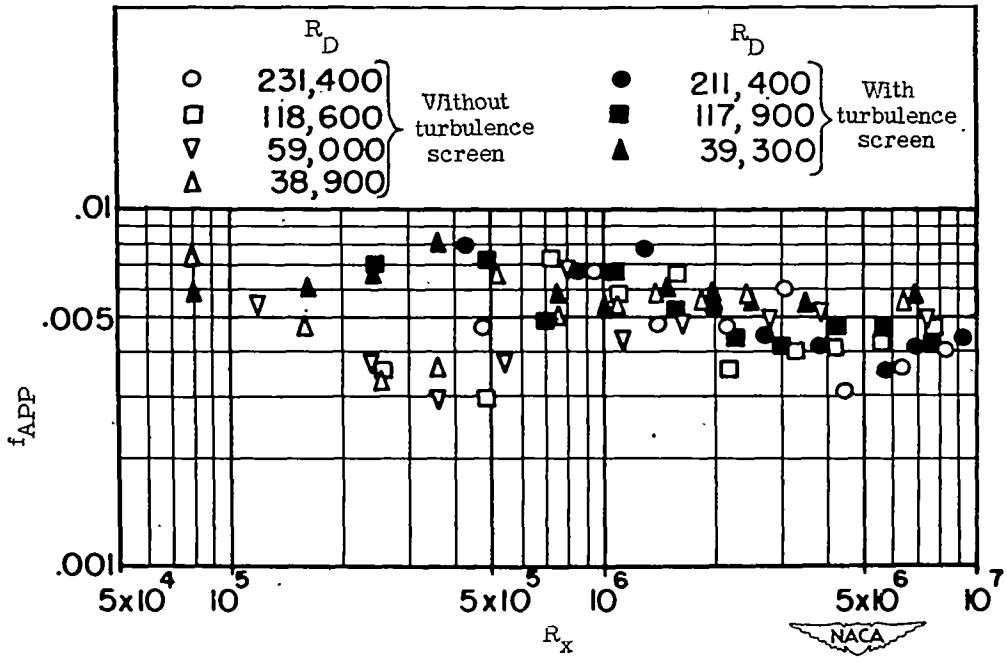

Figure 11.- Effect of induced turbulence (tube II, water tests). Local apparent friction coefficient against Reynolds number based on distance from inlet for constant values of Reynolds number based on diameter. Effect of wire screen (24-mesh, 30-gage) flush with downstream flange of calming chamber is shown.

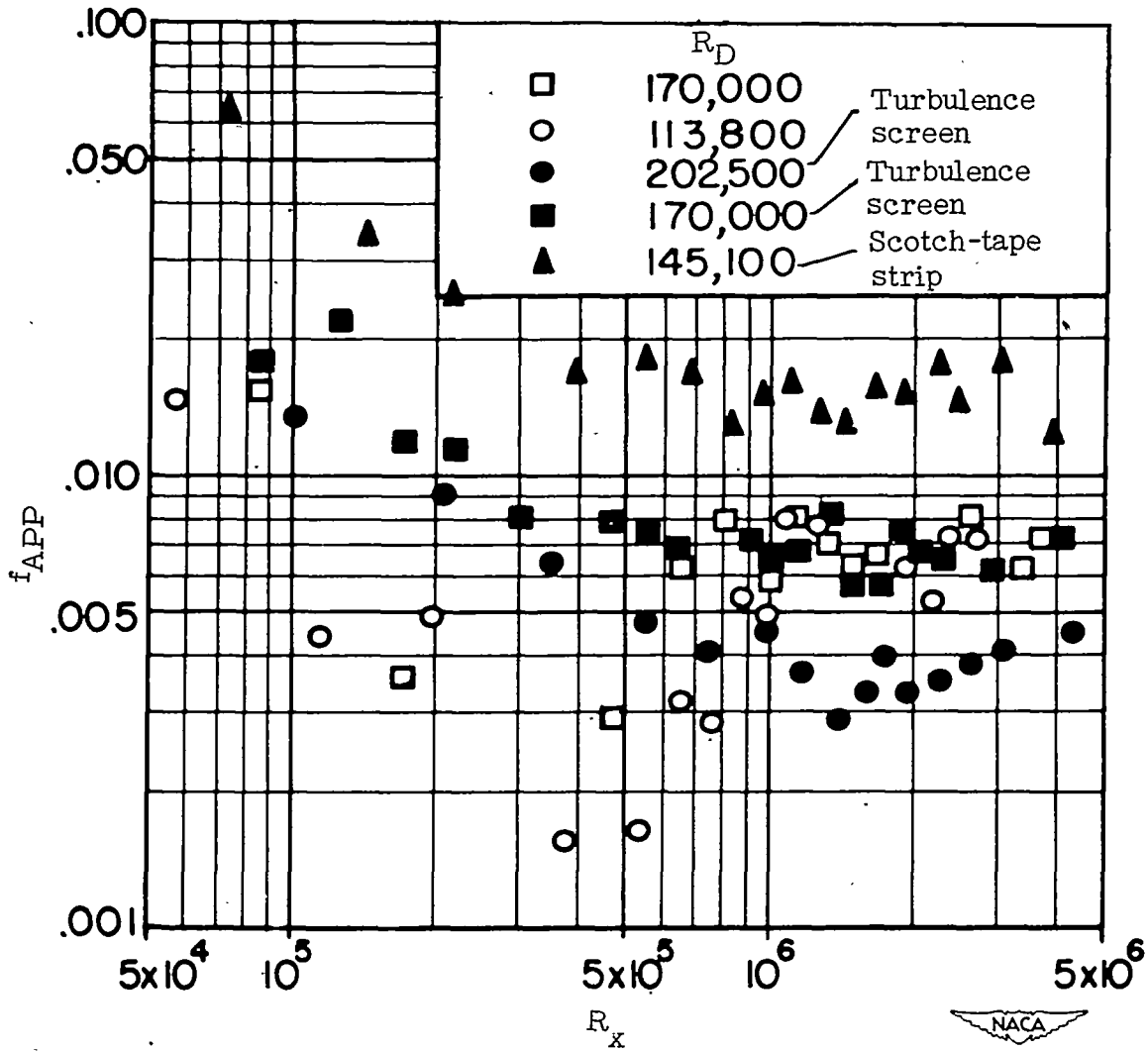

Figure 12.- Effect of induced turbulence (tube IV, air tests). Local apparent friction coefficient against Reynolds number based on distance from inlet for constant values of Reynolds number based on diameter. Effects of wire screen (24-mesh, 30-gage) across inlet and of strip of scotch tape $\left(\frac{1}{4}\text{ in. wide, } 0.0033\text{ in. thick}\right)$ at inlet are shown. Both screen and scotch tape were at the beginning of cylindrical section of tube.

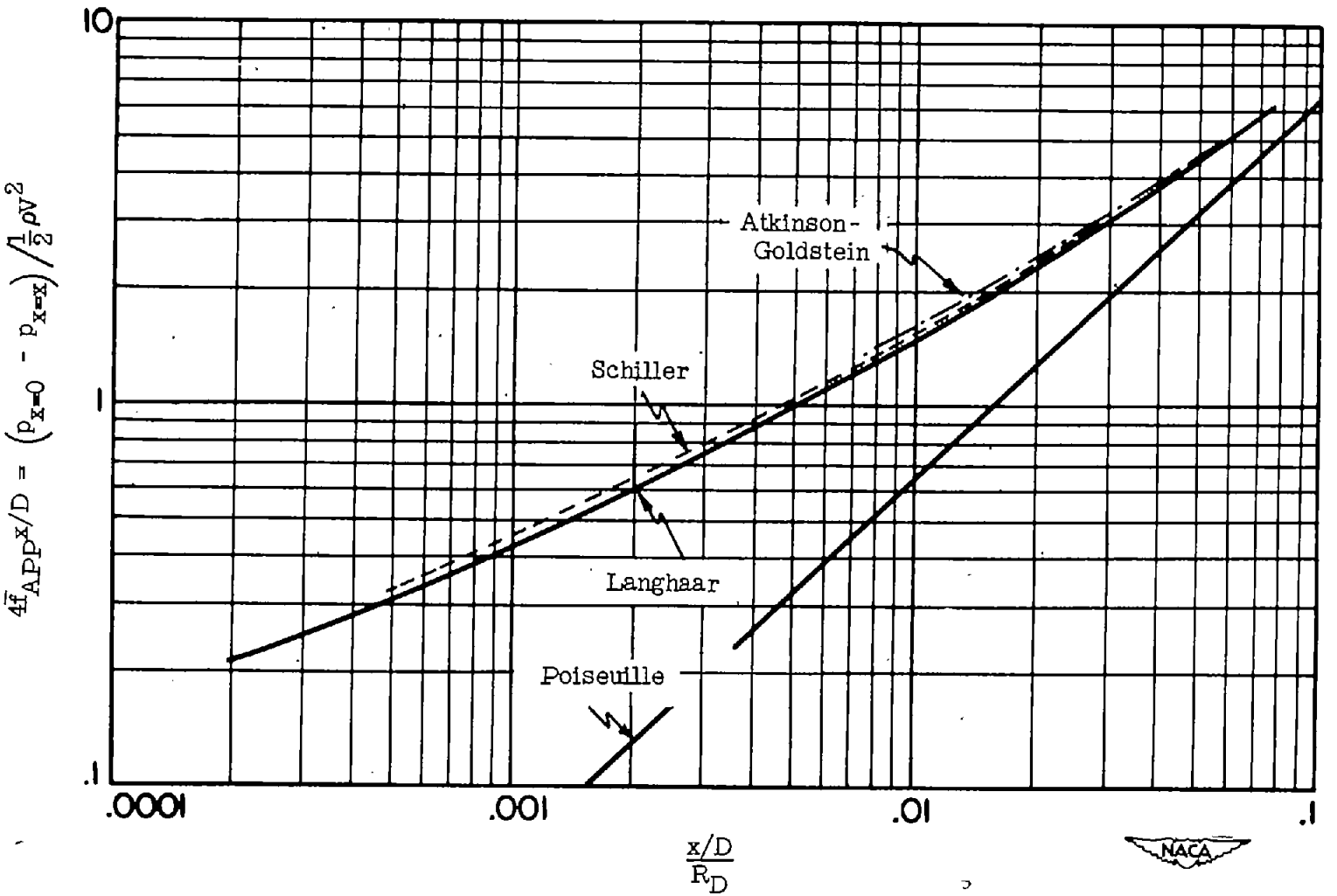

Figure 13.- Comparison of theories for laminar inlet region. Curves marked Langhaar, Schiller, and Atkinson-Goldstein are based on theories which take account of changing velocity profile. Curve marked Poiseuille is based on a parabolic velocity profile from beginning of inlet region.

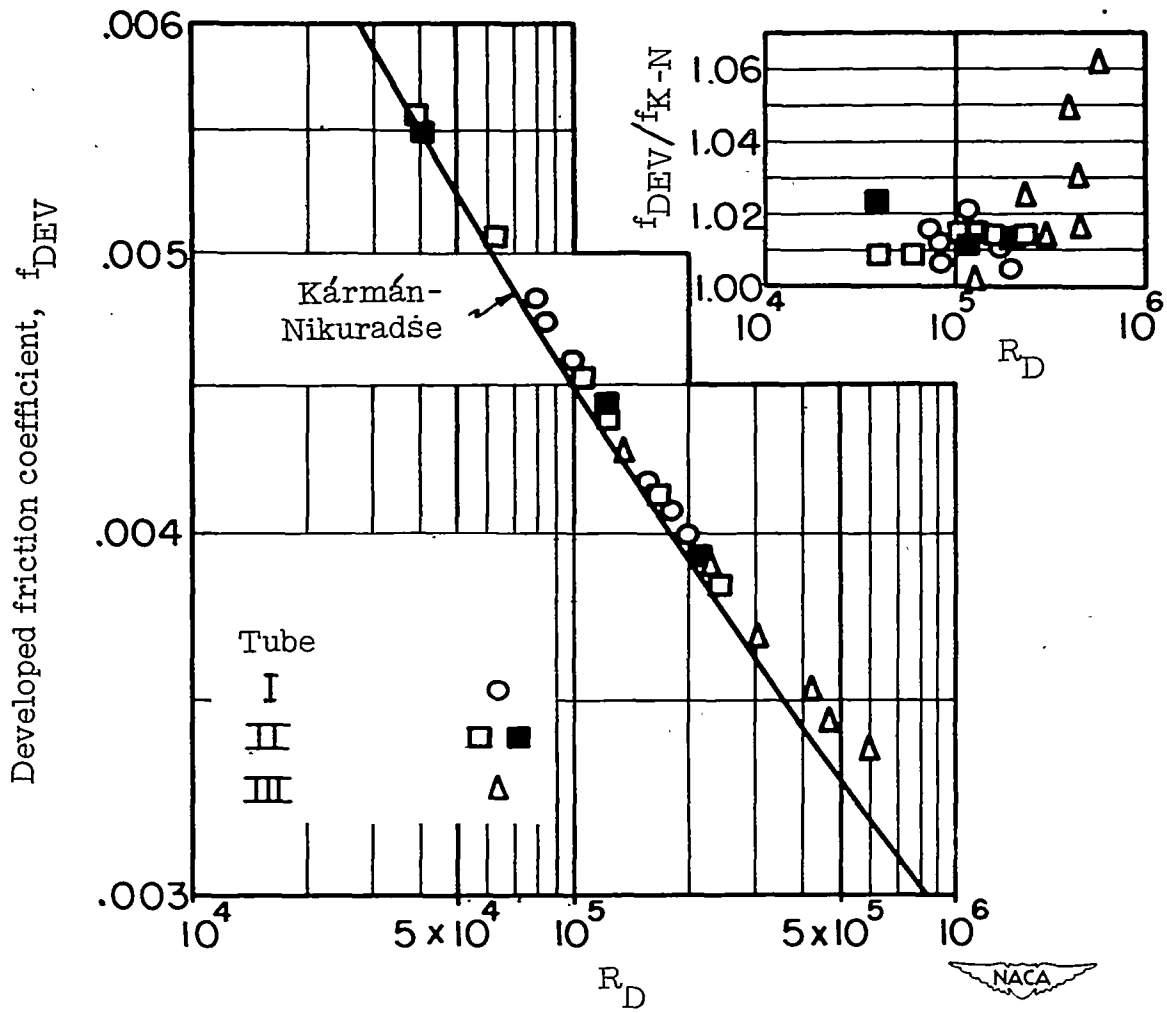

Figure 14.- Friction coefficients for water tests in region of unchanging velocity profile. Comparison between measured values of developed friction coefficient and values taken from Kármán-Nikuradse relation at same Reynolds number based on diameter. For tube II open squares represent runs with an undisturbed entrance, and closed squares represent runs with turbulence-inducing wire screen across inlet. The two values of x/D (x denotes distance from inlet; D denotes tube diameter) between which developed friction coefficient was measured were as follows: Tube I, from x/D = 168 to x/D = 200; tube II, from x/D = 72 to x/D = 237; tube III, from x/D = 44 to x/D = 126.

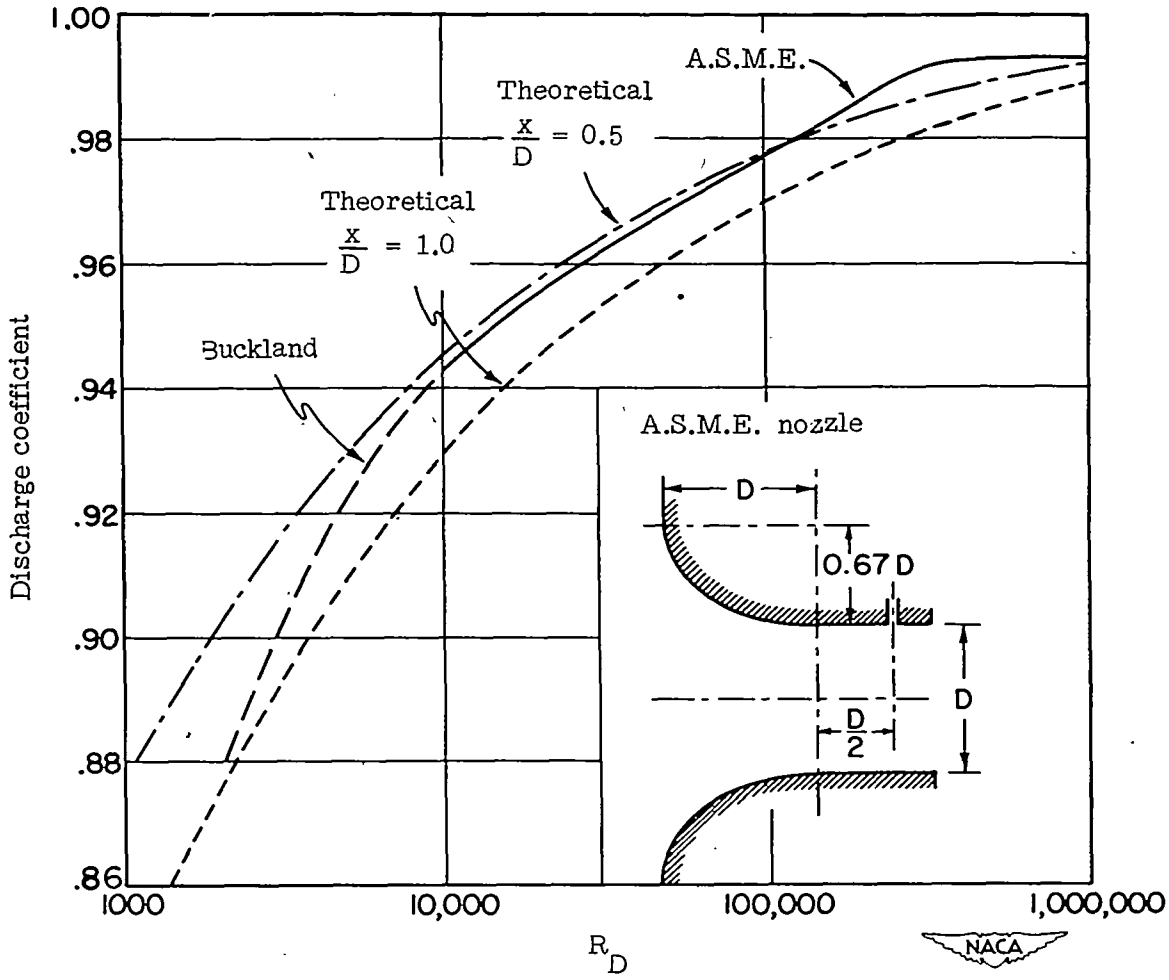

(a) Discharge coefficient against Reynolds number based on diameter. Curves marked A.S.M.E. and Buckland are from references 13 and 14, respectively, and refer to nozzles with cylindrical sections $\frac{1}{2}$ diameter in length. Theoretical curves were computed from equation (12) and figure 13.

Figure 15.- Comparison between predicted and published discharge coefficients for flow nozzles.

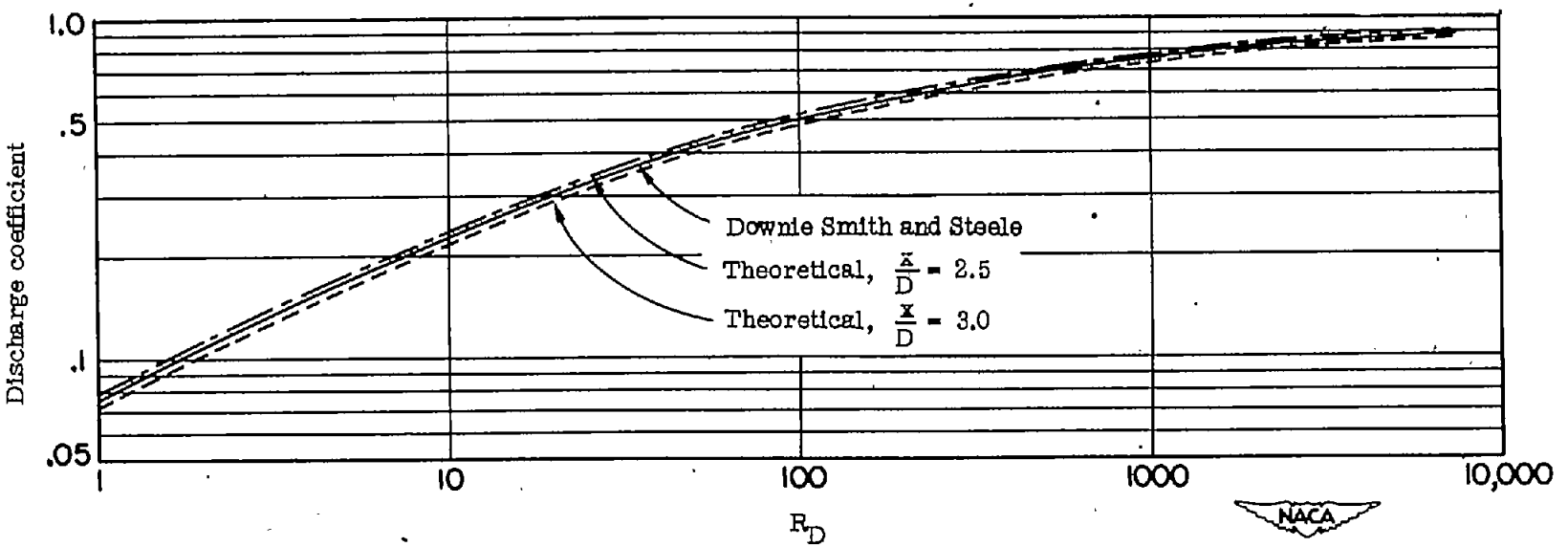

(b) Discharge coefficient against Reynolds number based on tube diameter. Curve marked Downie Smith and Steele is from reference 15 and refers to a nozzle with a cylindrical section $2\frac{1}{2}$ diameters in length. Theoretical curves were computed from equation (12) and figure 13.

Figure 15.- Concluded.